

## CHAPTER IV

### PARTIAL OXIDATION OF METHANE OVER Ni/CeO<sub>2</sub>-ZrO<sub>2</sub> CATALYSTS

#### 4.1 Abstract

In this study, methane partial oxidation (MPO) to synthesis gas over Ni/Ce<sub>1-x</sub>Zr<sub>x</sub>O<sub>2</sub> (x = 0, 0.25, and 1.0 with varying Ni loading of 5, 10 and 15 wt%) was investigated over the temperature range of 400-800°C. The experimental results showed that the catalysts prepared by impregnation method are more active than those prepared by gel impregnation method because of their higher degrees of metal dispersion and reducibility. Under the reaction conditions, MPO over Ni/CeO<sub>2</sub> and Ni/Ce<sub>0.75</sub>Zr<sub>0.25</sub>O<sub>2</sub> mixed oxide catalysts were active at temperatures above 550°C whereas that of Ni/ZrO<sub>2</sub> took place at temperatures above 650°C. The H<sub>2</sub>/CO molar ratio of 2.0±0.05 was obtained. Generally, the CH<sub>4</sub> conversion slightly increased while the CO and H<sub>2</sub> selectivities remained unchanged with increasing Ni loading. The Ni/Ce<sub>0.75</sub>Zr<sub>0.25</sub>O<sub>2</sub> mixed oxide catalysts were found to resist to coke formation more than the other catalysts due to their high degrees of metal dispersion and surface oxygen mobility. The TPO results indicated that a major source of carbon deposition on these catalysts is due to the methane decomposition.

#### 4.2 Introduction

In recent years, a catalytic partial oxidation of methane to synthesis gas (CO and H<sub>2</sub>) has been widely investigated as an attractive alternative process to steam reforming since the reaction is mildly exothermic and can produce H<sub>2</sub>/CO ratio of 2 which is suitable for methanol or Fischer-Tropsch synthesis.

Many catalysts containing transition metals (Ni, Cu and Fe) (Dissabayake *et al.*, 1991; Chellappa *et al.*, 1995; Au *et al.*, 1996; Hu and Ruckenstein, 1996; Lu *et al.*, 1998), noble metals (Ru, Rh, Pt and Pd) (Hickman and Schmidt, 1993; Boucouvalas *et al.*, 1994; Boucouvalas *et al.*, 1996; Mallens *et al.*, 1997; Otsuka *et al.*, 1999; Pantu *et al.*, 2000; Pantu and Gavalas, 2002) and metal oxides (Hargreaves

*et al.*, 1990; Irigoyen *et al.*, 1998; Otsuka *et al.*, 1998; Ruckenstein and Hu, 1999) were employed in investigations of methane partial oxidation. Among those, Ni-based catalyst shows an excellent catalytic activity for this reaction when compared to noble metal catalysts due to its low cost (Montoya *et al.*, 2000; Zhu and Flytzani-Stephanopoulos, 2001). However, Ni is deactivated easily by coke deposition and/or metal sintering.

Carbon deposition on a supported Ni catalyst mainly comes from methane decomposition and CO disproportionation reaction at high temperatures. In general, the deposition of carbon would occur over the metallic sites as well as on the acid sites of the support. Therefore, the studies of highly active and stable catalyst have been focused. Many additives were successive to reduce carbon deposition for Ni- $\text{Al}_2\text{O}_3$  such as Li, La, K and Na (Miao *et al.*, 1997). The use of Ni on different supports such as CaO,  $\text{SiO}_2$  and MgO was also reported (Au *et al.*, 1996; Tang *et al.*, 1998). It was reported that the use of supports in the presence of basic sites such as MgO resulted in enhancing activities and lowering carbon deposition (Tang *et al.*, 1998). On the other hand, use of reducibility support could result in enhancing further activity and decreasing coke deposition (Swann *et al.*, 1994; Pantu and Gavalas, 2002; Noronha *et al.*, 2001). Stagg-Williams *et al.* (2000) reported that a higher degree of reduction of catalyst resulted in an increase in oxygen vacancies, thus subsequent resisting to carbon deposition.

Recently, Otsuka *et al.* (1998) has reported that  $\text{CeO}_2$  could be able to convert methane to synthesis gas with a  $\text{H}_2/\text{CO}$  ratio of 2 and showed that adding Pt black could promote a syngas formation rate. This finding was similar to Ni/ $\text{CeO}_2$  reported by Dong *et al.* (2002). They also proposed a mechanism over Ni/ $\text{CeO}_2$  that  $\text{CH}_4$  dissociates on Ni and the resultant carbon species quickly migrate to the interface of Ni- $\text{CeO}_2$  and then react with lattice oxygen of  $\text{CeO}_2$  to form CO. However, ceria still has some disadvantages. Ceria, by itself, has a poor thermal resistance and stability at high temperatures. Ceria-supported Ni with high Ni loading (13 wt%) was an active catalyst for methane partial oxidation but rapidly deactivated by carbon deposition (Tang *et al.*, 1998).

The addition of  $\text{ZrO}_2$  to  $\text{CeO}_2$  can improve its oxygen storage capacity, redox properties, thermal resistance and better catalytic activity at low temperatures

(Fornasiero *et al.*, 1995; Fornasiero *et al.*, 1996; Hori *et al.*, 1998; Gonzalez-Velasco *et al.*, 1999; Roh *et al.*, 2002). It was demonstrated that CeO<sub>2</sub>-ZrO<sub>2</sub> mixed oxides produced synthesis gas with a H<sub>2</sub>/CO ratio of 2 and the formation rates of H<sub>2</sub> and CO were increased due to the incorporation of ZrO<sub>2</sub> into CeO<sub>2</sub>. The oxygen desorption and reduction by H<sub>2</sub> of Ce<sub>1-x</sub>Zr<sub>x</sub>O<sub>2</sub> solid solution with  $x \leq 0.5$  took place at lower temperature as compared with pure ceria. In our early study, we have also found that Ce<sub>0.75</sub>Zr<sub>0.25</sub>O<sub>2</sub> solid solution exhibited the highest reducibility (Pengpanich *et al.*, 2002). On the contrary, it was demonstrated that Ni/CeO<sub>2</sub>-ZrO<sub>2</sub> with Ce/Zr ratio of 0.25 or small amount of CeO<sub>2</sub> and exhibited high catalytic activity methane partial oxidation (Takeguchi *et al.*, 2001; Dong *et al.*, 2002).

In this study, we report on the activity, selectivity and stability of Ni/Ce<sub>0.75</sub>Zr<sub>0.25</sub>O<sub>2</sub> catalyst compared with Ni/CeO<sub>2</sub> and Ni/ZrO<sub>2</sub> catalysts for methane partial oxidation to synthesis gas over the temperature range of 400-800°C at atmospheric pressure.

## 4.3 Experimental

### 4.3.1 Catalyst Preparation

Mixed oxide solid solutions of Ce-Zr metals were prepared as catalyst supports via urea hydrolysis. The Ce-Zr mixed oxide solid solution samples were prepared from Ce(NO<sub>3</sub>)<sub>3</sub>·6H<sub>2</sub>O (99.0%, Fluka) and ZrOCl<sub>2</sub>·8H<sub>2</sub>O (99.0%, Fluka). The ratio between the metal salts was altered depending on the desired solid solution concentration: Ce<sub>1-x</sub>Zr<sub>x</sub>O<sub>2</sub> in which  $x = 0, 0.25$  and  $1.0$ . The synthesized procedure has been reported elsewhere (Pengpanich *et al.*, 2002).

The catalysts prepared by the incipient wetness impregnation method were designated as IMP. To prepare Ni/Ce<sub>1-x</sub>Zr<sub>x</sub>O<sub>2</sub> (IMP) catalysts, Ni (5, 10 and 15 wt%) was loaded by the incipient wetness impregnation method into the supports using its nitrate salt solution.

The catalysts designated as GEL were prepared by the gel impregnation method. In the case of GEL catalysts, a 5wt% Ni was loaded during the gel step. The washed gel was added with nickel nitrate salt solution to obtain a desired loading

before drying and calcination. The catalysts were then calcined at 500°C for 4 hr in air.

#### 4.3.2 Catalyst Characterizations

BET surface area was determined by N<sub>2</sub> adsorption at 77 K (a five point Brunauer-Emmett-Teller (BET) method using a Quantachrome Corporation Autosorb). Prior to the analysis, the samples were outgassed to eliminate volatile adsorbents on the surface at 250°C for 4 hr.

H<sub>2</sub> uptake and degree of dispersion were determined by pulse technique using a temperature programmed analyzer (ThermoFinnigan modeled TPDRO 1100). Prior to pulse chemisorption, the sample was reduced in H<sub>2</sub> atmosphere at 500°C for 1 hr. Then the sample was purged with N<sub>2</sub> at 500°C for 30 min and cooled down to 40°C in flowing N<sub>2</sub>. A H<sub>2</sub> pulse (99.99% H<sub>2</sub> with a sample loop volume of 0.4 ml) was injected into the sample at 40°C.

An X-ray diffractometer (XRD) system (Rigaku) equipped with a RINT 2000 wide-angle goniometer using CuK<sub>α</sub> radiation and a power of 40 kV x 30 mA was used for examination of the crystalline structure. The intensity data were collected at 25 °C over a 2θ range of 20-90° with a scan speed of 5° (2θ)/min and a scan step of 0.02° (2θ).

The morphology of carbon deposition on the spent catalysts was observed by transmission electron microscopy (TEM) with a JEOL (JEM-2010) transmission electron microscope operated at 200 kV. The samples were dispersed in absolute ethanol ultrasonically, and the solutions were then dropped on copper grids coated with a lacey carbon film.

H<sub>2</sub> temperature programmed reduction (H<sub>2</sub>-TPR) experiments were carried out using a TPR analyzer (ThermoFinnigan modeled TPDRO 1100). The sample was pretreated in N<sub>2</sub> atmosphere at 400°C for 30 min prior to running the TPR experiment, and then cooled down to room temperature in N<sub>2</sub>. A 5% H<sub>2</sub>/N<sub>2</sub> gas was used as a reducing gas. The sample temperature was raised at a constant rate of 10°C/min from room temperature to 950°C. The amount of H<sub>2</sub> consumption as a function of temperature was determined from a TCD signal.

CH<sub>4</sub> temperature programmed reduction (CH<sub>4</sub>-TPR) experiments were carried out in a quartz micro-reactor in a similar manner to H<sub>2</sub>-TPR experiments but using a 2% CH<sub>4</sub> balanced with He as a reducing gas. The effluent gas composition as a function of temperature was measured using a mass spectrometer (Balzer Instruments modeled Thermostar GSD 300T).

Temperature programmed oxidation (TPO) carried out in a TPO micro-reactor analyzer coupled with an FID was used to quantify the amount of coke formation in the spent catalysts. Typically, a 40 mg sample was heated from room temperature in flowing 2% O<sub>2</sub>/He at a heating rate of 10°C/min to 900°C. The output gas was passed to a methanation reactor using 15 wt% Ni/Al<sub>2</sub>O<sub>3</sub> as a catalyst. After the TPO system reached 900°C, where all carbon had been burned off, the FID signal for methane was calibrated by injecting 100 µl of CO<sub>2</sub> pulses into the methanation reactor, and sending the methane produced into the FID. By integrating the methane signal during the entire TPO run, it was possible to calculate the amount of coke removed from catalyst.

#### 4.3.3 Catalytic Activity Tests

Catalytic activity tests for methane partial oxidation were carried out in a packed-bed quartz microreactor (i.d. Ø 6 mm). Typically, a 100 mg catalyst sample was packed between the layers of quartz wool. The reactor was placed in an electric furnace equipped with K-type thermocouples. The catalyst bed temperature was monitored and controlled by Shinko temperature controllers. The feed gas mixture containing 4%CH<sub>4</sub>, 2%O<sub>2</sub> and balanced with He was used for which a gas hourly space velocity (GHSV) was maintained at 53,000 hr<sup>-1</sup> using Brooks mass flow controllers. Measurements were carried out at various furnace temperatures adjusted sequentially from 400-800°C with an interval of 50°C. The carbon formations on the catalysts were further studied in the same system as for MPO at 700-800°C with different conditions (GHSV of 53,000 hr<sup>-1</sup> and CH<sub>4</sub>/O<sub>2</sub> ratios of 1.6, 2.0 and 2.5).

The gaseous products were chromatographically analyzed using a Shimadzu GC 8A fitted with a TCD. A CTR I (Alltech) packed column was used to separate all products at 50°C except for H<sub>2</sub>O which was trapped out prior to entering

the column. The CH<sub>4</sub> conversion ( $X_{\text{CH}_4}$ ), O<sub>2</sub> consumption ( $X_{\text{O}_2}$ ) and selectivity (S) that reported in this work were calculated as follows:

$$\% X_{\text{CH}_4} = \frac{\text{CH}_4^{\text{in}} - \text{CH}_4^{\text{out}}}{\text{CH}_4^{\text{in}}} \times 100 \quad (3.3)$$

$$\% X_{\text{O}_2} = \frac{\text{O}_2^{\text{in}} - \text{O}_2^{\text{out}}}{\text{O}_2^{\text{in}}} \times 100 \quad (3.4)$$

$$\% S_{\text{CO}} = \frac{\text{CO}^{\text{out}}}{\text{CO}^{\text{out}} + \text{CO}_2^{\text{out}}} \times 100 \quad (3.5)$$

$$\% S_{\text{H}_2} = \frac{\text{H}_2^{\text{out}}}{\text{H}_2^{\text{out}} + \text{H}_2\text{O}^{\text{out}}} \times 100 \quad (3.6)$$

## 4.4 Results and Discussion

### 4.4.1 Catalyst Characterizations

#### 4.4.1.1 BET Surface Area, H<sub>2</sub> Uptake and Metal Dispersion

The BET surface areas, H<sub>2</sub> uptake and metallic Ni dispersion of the catalysts are shown in Table 4.1. The surface areas of the catalysts are in the range of 80-138 m<sup>2</sup>/g. For IMP catalysts, the surface areas were found to decrease with increasing Ni loading. When Ni loading was increased from 5 to 15 wt%, Ni/CeO<sub>2</sub> (IMP) surface areas were drastically decreased by about 40%. On the other hand, the surface areas of Ni/Ce<sub>0.75</sub>Zr<sub>0.25</sub>O<sub>2</sub> (IMP) and Ni/ZrO<sub>2</sub> (IMP) catalysts were somewhat decreased by 17 and 8%, respectively. This might be due to nickel acts as a nucleating agent promoting the sintering and ceria, itself, has low thermal stability (Montoya *et al.*, 2000). The surface areas of GEL catalysts are barely different from those of IMP catalysts.

The degree of dispersion of Ni/CeO<sub>2</sub> and Ni/Ce<sub>0.75</sub>Zr<sub>0.25</sub>O<sub>2</sub> catalysts are higher than those of Ni/ZrO<sub>2</sub> catalysts indicating that Ni particles are better dispersed on CeO<sub>2</sub> and Ce<sub>0.75</sub>Zr<sub>0.25</sub>O<sub>2</sub> than ZrO<sub>2</sub>. The dispersion degree was found to decrease with an increase in metal loading. This is due to the formation of NiO bulk particles. It should be noted that the amount of H<sub>2</sub> uptake for the GEL catalysts is lower than that for IMP catalysts indicating a lower exposed Ni metal due to particle encapsulation (Shishido *et al.*, 2002).

#### 4.4.1.2 XRD Analysis

The structure of the catalysts was determined using an XRD as shown in Figure 4.1. For 5% Ni loading catalysts, the XRD patterns of Ni/CeO<sub>2</sub> and Ni/Ce<sub>0.75</sub>Zr<sub>0.25</sub>O<sub>2</sub> prepared via both IMP and GEL methods exhibited a cubic fluorite structure while the XRD patterns of both the IMP and GEL Ni/ZrO<sub>2</sub> catalysts showed a tetragonal structure. No separate Ni and NiO phases were found by XRD for such a low Ni loading (5 wt% Ni). It might be postulated that the amount of Ni metal loading is too small to be detected by the XRD. At higher Ni loadings (10 and 15 wt% Ni), three new peaks at about 37°, 43° and 62° (2θ) indicating a NiO phase were observed. The peak intensity was obviously stronger with increasing Ni loading suggesting that at a low Ni content, NiO was present in the form of nanoparticles while at a high Ni content, bulk NiO agglomerated particles were present (Zhu and Flytzani-Stephanopoulos, 2001). This result appears to be in good agreement with the degree of metal dispersion data.

**Table 4.1** BET surface area, H<sub>2</sub> uptake and degree of dispersion of the catalysts

Catalyst	BET Surface Area (m <sup>2</sup> /g)	H <sub>2</sub> Uptake (μmol/g)	Dispersion (%)
5% Ni/CeO <sub>2</sub> (IMP)	135	34.83	8.20
5% Ni/Ce <sub>0.75</sub> Zr <sub>0.25</sub> O <sub>2</sub> (IMP)	112	39.74	9.33
5% Ni/ZrO <sub>2</sub> (IMP)	138	4.12	0.97
10% Ni/CeO <sub>2</sub> (IMP)	114	33.66	3.95
10% Ni/Ce <sub>0.75</sub> Zr <sub>0.25</sub> O <sub>2</sub> (IMP)	95	31.04	3.64
10% Ni/ZrO <sub>2</sub> (IMP)	128	3.88	0.46
15% Ni/CeO <sub>2</sub> (IMP)	65	33.61	2.60
15% Ni/Ce <sub>0.75</sub> Zr <sub>0.25</sub> O <sub>2</sub> (IMP)	93	31.61	2.50
15% Ni/ZrO <sub>2</sub> (IMP)	127	3.47	0.27
5% Ni/CeO <sub>2</sub> (GEL)	128	19.95	4.69
5% Ni/Ce <sub>0.75</sub> Zr <sub>0.25</sub> O <sub>2</sub> (GEL)	104	6.17	1.45
5% Ni/ZrO <sub>2</sub> (GEL)	124	1.28	0.30



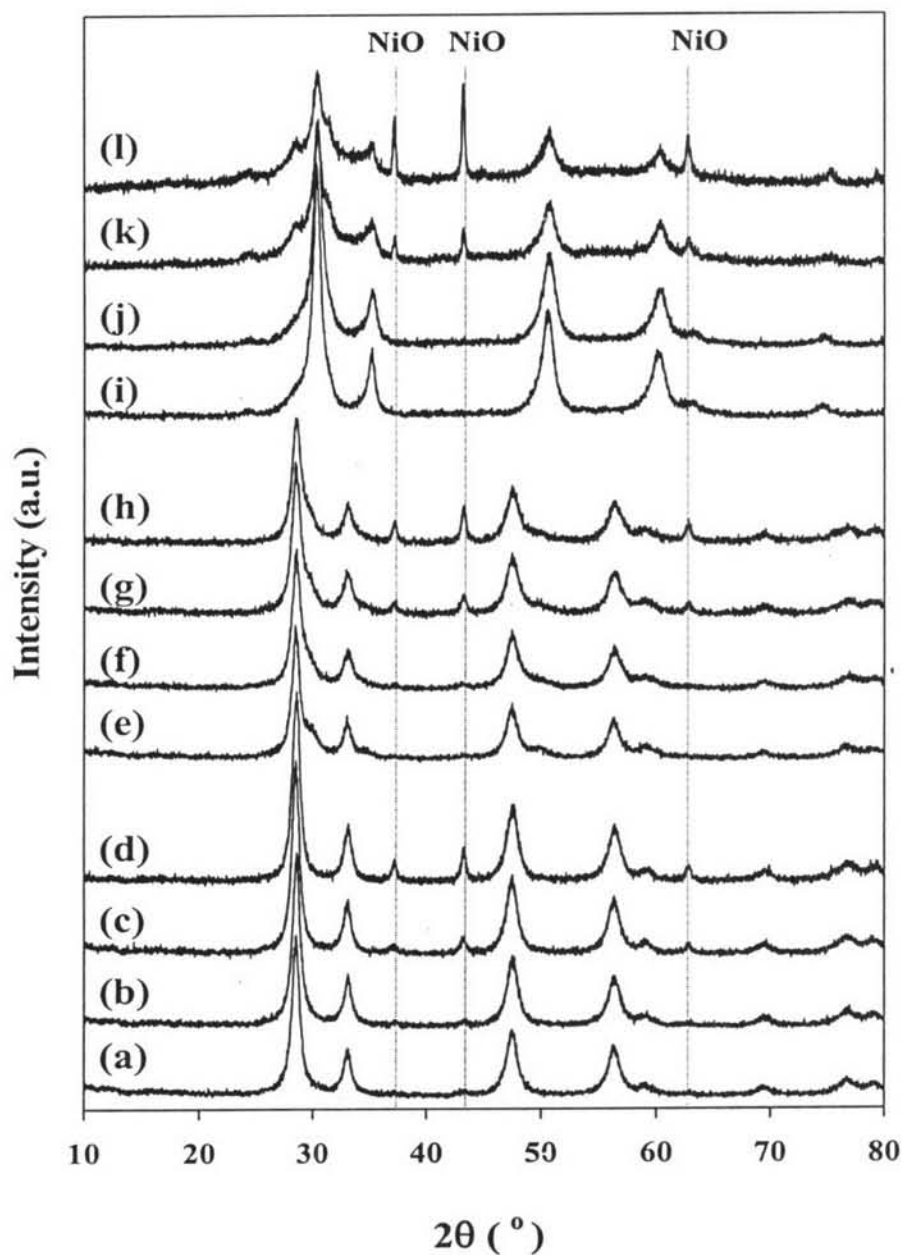


**Figure 4.1** XRD patterns of catalysts calcined at 500°C: (a) 5 wt.% Ni/CeO<sub>2</sub> (GEL), (b) 5 wt.% Ni/CeO<sub>2</sub> (IMP), (c) 10 wt.% Ni/CeO<sub>2</sub> (IMP), (d) 15 wt.% Ni/CeO<sub>2</sub> (IMP), (e) 5 wt.% Ni/Ce<sub>0.75</sub>Zr<sub>0.25</sub>O<sub>2</sub> (GEL), (f) 5 wt.% Ni/Ce<sub>0.75</sub>Zr<sub>0.25</sub>O<sub>2</sub> (IMP), (g) 10 wt.% Ni/Ce<sub>0.75</sub>Zr<sub>0.25</sub>O<sub>2</sub> (IMP), (h) 15 wt.% Ni/Ce<sub>0.75</sub>Zr<sub>0.25</sub>O<sub>2</sub> (IMP), (i) 5 wt.% Ni/ZrO<sub>2</sub> (GEL), (j) 5 wt.% Ni/ZrO<sub>2</sub> (IMP), (k) 10 wt.% Ni/ZrO<sub>2</sub> (IMP), (l) 15 wt.% Ni/ZrO<sub>2</sub> (IMP).

#### 4.4.1.3 H<sub>2</sub>-TPR

The H<sub>2</sub>-TPR profiles of the 5 wt% Ni IMP catalysts compared with their supports are shown in Figure 4.2. For the Ni/CeO<sub>2</sub> (IMP) catalysts, a strong peak with the maximum temperature at ca. 360°C and another broad peak with the maximum temperature at ca. 800°C were observed. The first peak was attributed to the reduction of NiO (indicated by XRD analysis) to Ni<sup>0</sup> and the other peak is related to the bulk reduction of CeO<sub>2</sub> from Ce<sup>+4</sup> to Ce<sup>+3</sup> (Montoya *et al.*, 2000; Takeguchi *et al.*, 2001).

Figure 4.3 shows the H<sub>2</sub>-TPR profiles of 5, 10 and 15 wt% Ni IMP catalysts. An increase in Ni loading does not affect the reduction temperature of NiO over CeO<sub>2</sub> but a small peak with the maximum temperature at ca. 250°C was observed for the 10 and 15 wt% Ni loadings. This peak might be due to the reduction of NiO particles with interacting weakly with support (Roh *et al.*, 2002) or hydrogen spillover effect (Takeguchi *et al.*, 2001). Similar results were found in the case of Ni/Ce<sub>0.75</sub>Zr<sub>0.25</sub>O<sub>2</sub> (IMP) catalysts which exhibit two peaks with the maxima at ca. 360 and 800°C. However, a small peak at ca. 250°C was smaller than that of Ni/CeO<sub>2</sub> indicating a lower amount of free NiO particles. This suggests that NiO-support interactions for Ni/Ce<sub>0.75</sub>Zr<sub>0.25</sub>O<sub>2</sub> (IMP) catalysts be stronger than those for Ni/CeO<sub>2</sub> (IMP) catalysts. For the 5 wt% Ni/ZrO<sub>2</sub> (IMP) catalyst, a peak at temperature ca. 480°C was observed while no reduction of ZrO<sub>2</sub> was observed (Figure 4.2). As an increase in Ni loading (10 and 15 wt%), the unresolved peak with the maximum temperature at ca. 350°C was observed. This suggests that there be two kinds of NiO species. The peak at a lower temperature is assigned to a free NiO species interacting weakly with support, and the other peak at a higher temperature is attributed to a complex NiO species interacting strongly with support (Roh *et al.*, 2002).

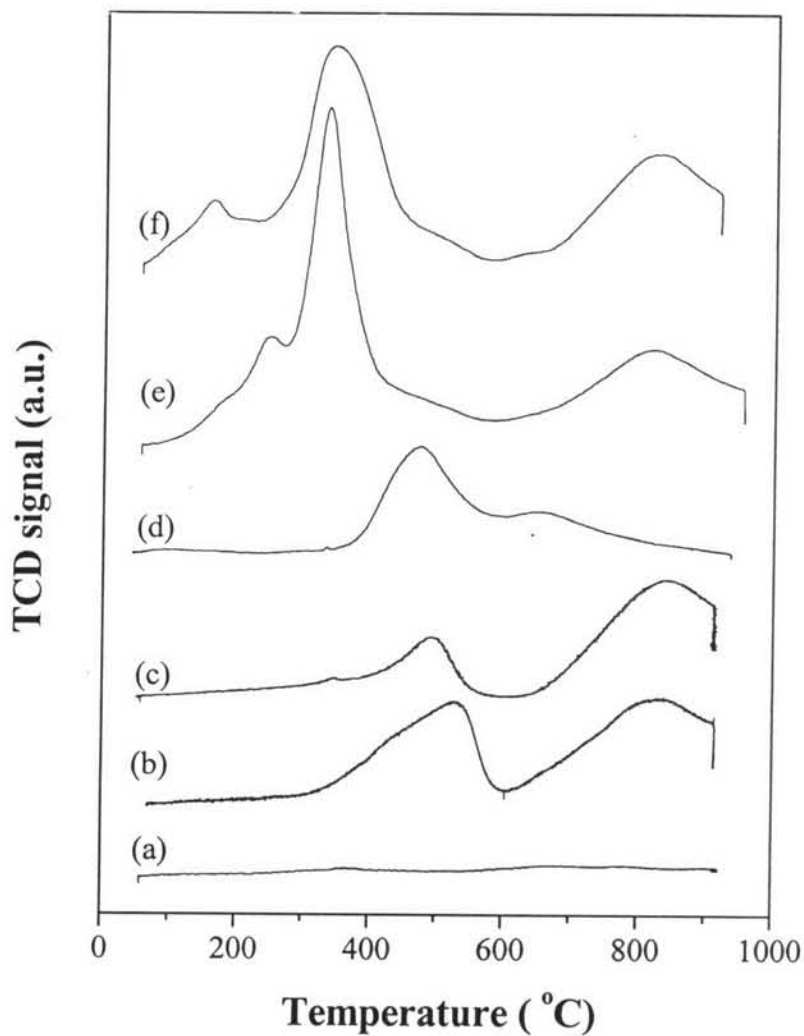


**Figure 4.2**  $\text{H}_2$ -TPR profiles of IMP catalysts and their supports calcined at  $500^\circ\text{C}$  with a heating rate of  $10^\circ\text{C min}^{-1}$ , a reducing gas containing 5% hydrogen in nitrogen with a flow rate of  $30 \text{ ml min}^{-1}$ : (a)  $\text{ZrO}_2$  (b)  $\text{Ce}_{0.75}\text{Zr}_{0.25}\text{O}_2$  (c)  $\text{CeO}_2$  (d) 5 wt%  $\text{Ni}/\text{ZrO}_2$  (e) 5 wt%  $\text{Ni}/\text{Ce}_{0.75}\text{Zr}_{0.25}\text{O}_2$  and (f) 5 wt%  $\text{Ni}/\text{CeO}_2$ .

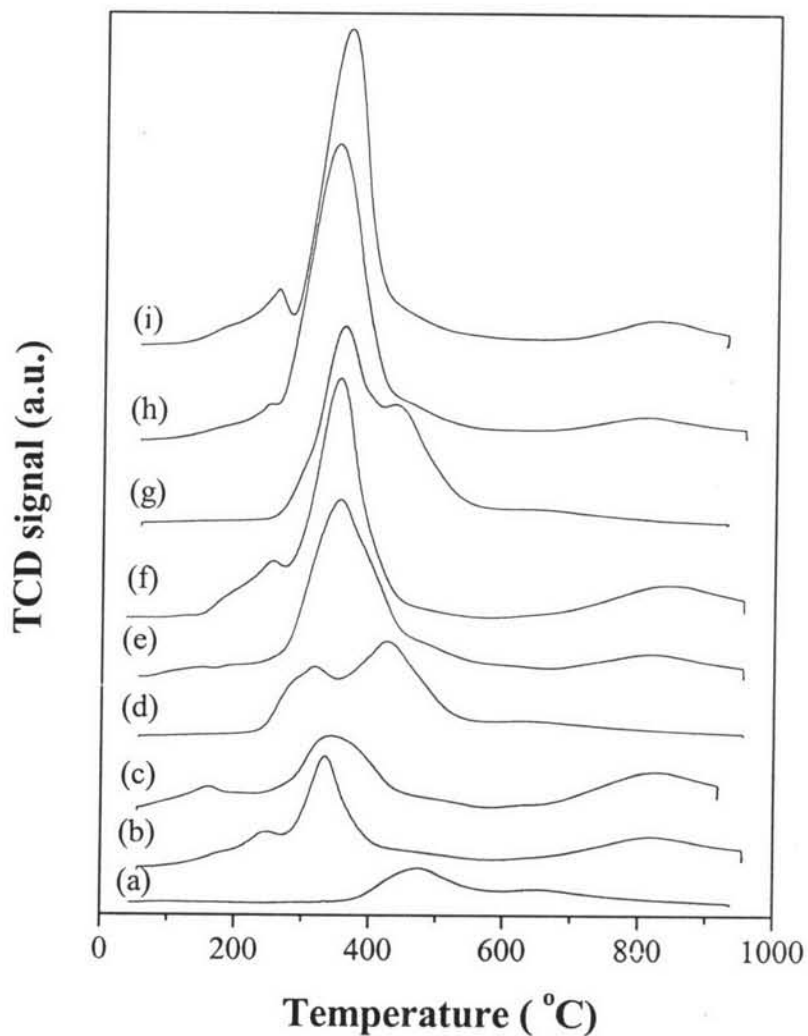


**Figure 4.3**  $\text{H}_2$ -TPR profiles of IMP catalysts calcined at  $500^\circ\text{C}$  with a heating rate of  $10^\circ\text{C min}^{-1}$ , a reducing gas containing 5% hydrogen in nitrogen with a flow rate of  $30 \text{ ml min}^{-1}$ : (a) 5 wt% Ni/ $\text{ZrO}_2$  (b) 5 wt% Ni/ $\text{Ce}_{0.75}\text{Zr}_{0.25}\text{O}_2$  (c) 5 wt% Ni/ $\text{CeO}_2$  (d) 10 wt% Ni/ $\text{ZrO}_2$  (e) 10 wt% Ni/ $\text{Ce}_{0.75}\text{Zr}_{0.25}\text{O}_2$  (f) 10 wt% Ni/ $\text{CeO}_2$  (g) 15 wt% Ni/ $\text{ZrO}_2$  (h) 15 wt% Ni/ $\text{Ce}_{0.75}\text{Zr}_{0.25}\text{O}_2$  and (i) 15 wt% Ni/ $\text{CeO}_2$ .

The H<sub>2</sub>-TPR profiles for the GEL catalysts are similar to those for the IMP catalysts as shown in Figure 4.4. However, the reduction profile of 5%Ni/Ce<sub>0.75</sub>Zr<sub>0.25</sub>O<sub>2</sub> (GEL) is slightly different from that of the IMP catalyst. The catalysts prepared by gel impregnation show a broader reduction peak than those prepared by incipient wetness impregnation. The wideness of peak is due to a broad particle size distribution. Also the GEL reduction temperature is relatively higher than the IMP catalysts. Interestingly, the reduced NiO region of 5%Ni/Ce<sub>0.75</sub>Zr<sub>0.25</sub>O<sub>2</sub> (GEL) was shifted from the maximum at ca. 350°C to 420°C when compared with that of 5%Ni/Ce<sub>0.75</sub>Zr<sub>0.25</sub>O<sub>2</sub> (IMP) catalyst. This result indicates that the catalyst prepared by gel impregnation has a higher interaction between NiO and support (Montoya *et al.*, 2000).

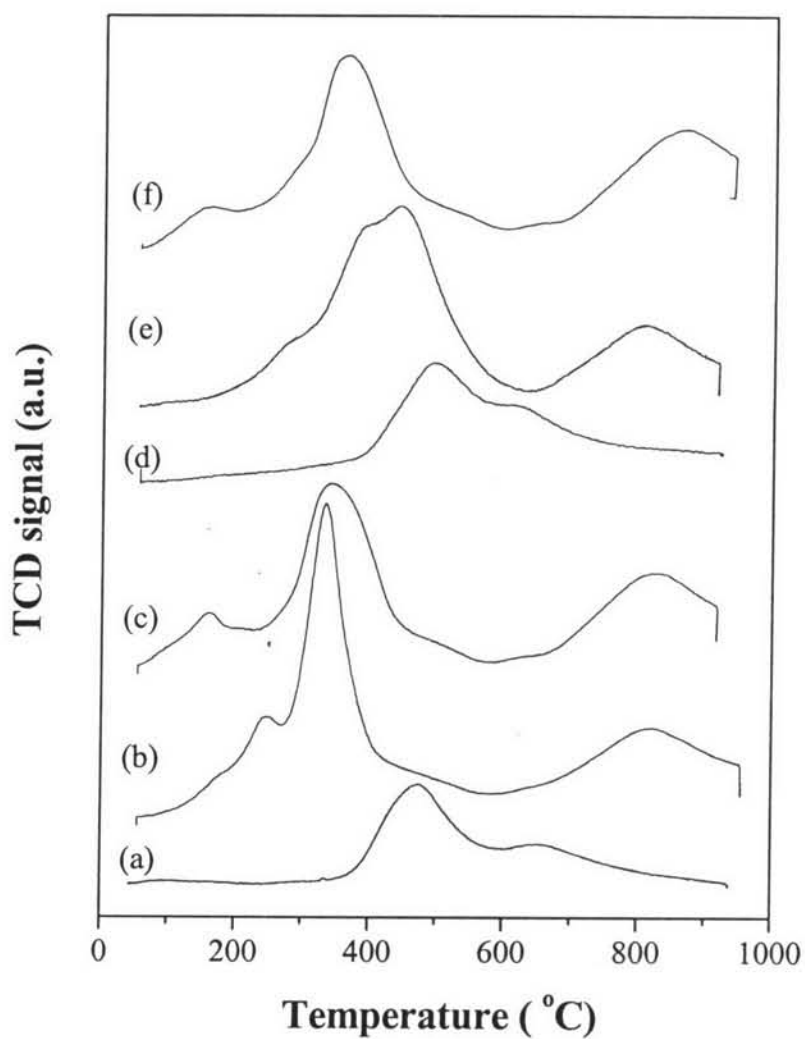


**Figure 4.4**  $H_2$ -TPR profiles of IMP and GEL catalysts calcined at  $500^\circ C$  with a heating rate of  $10^\circ C \text{ min}^{-1}$ , a reducing gas containing 5% hydrogen in nitrogen with a flow rate of  $30 \text{ ml min}^{-1}$ : (a) 5 wt% Ni/ $ZrC_2$  (IMP) (b) 5 wt% Ni/ $Ce_{0.75}Zr_{0.25}O_2$  (IMP) (c) 5 wt% Ni/ $CeO_2$  (IMP) (d) 5 wt% Ni/ $ZrO_2$  (GEL) (e) 5 wt% Ni/ $Ce_{0.75}Zr_{0.25}O_2$  (GEL) and (f) 5 wt% Ni/ $CeO_2$  (GEL).

#### 4.4.2 Catalytic Activity for Methane Partial Oxidation

##### 4.4.2.1 *Catalytic Activity Test*

Figures 4.5–4.7 show the CH<sub>4</sub> conversion, CO selectivity and H<sub>2</sub> selectivity of MPO over the Ni/CeO<sub>2</sub>, Ni/Ce<sub>0.75</sub>Zr<sub>0.25</sub>O<sub>2</sub> and Ni/ZrO<sub>2</sub> catalysts. The catalytic activity for MPO to synthesis gas was tested in a dilute mixture (4%CH<sub>4</sub> and 2%O<sub>2</sub> balanced with He) in the temperature range of 400-800°C. The supports (CeO<sub>2</sub>, Ce<sub>0.75</sub>Zr<sub>0.25</sub>O<sub>2</sub> and ZrO<sub>2</sub>) are not relatively active for MPO as seen in Figures 4.5-4.7. Dominant MPO products (CO and H<sub>2</sub>) were observed at temperatures higher than 600°C with only about 5% CO yield at 700°C.

The addition of Ni onto the supports resulted in an increase in MPO catalytic activity. As shown in Figure 4.5-4.7, for the 5 wt% IMP catalysts, CH<sub>4</sub> conversion with the complete oxidation products, CO<sub>2</sub> and H<sub>2</sub>O, was observed at temperatures < 550°C for Ni/CeO<sub>2</sub> and Ni/Ce<sub>0.75</sub>Zr<sub>0.25</sub>O<sub>2</sub> catalysts and at temperatures < 650°C for Ni/ZrO<sub>2</sub> catalyst. Beyond such temperatures, the CH<sub>4</sub> conversion dramatically increases resulting from the methane partial oxidation reaction. The oxygen was completely consumed and the H<sub>2</sub>/CO molar ratio of ca. 2.0±0.05 was obtained at these conditions. The results are similar to that observed by Shishido *et al.* (2002) suggesting that the first stage is corresponding to the combustion of methane followed by steam and CO<sub>2</sub> reforming reactions of methane to synthesis gas.

As illustrated in Figures 4.5–4.7, CH<sub>4</sub> conversion and CO selectivity at 700°C are about 92% and 96%, respectively, over 5 wt% Ni/CeO<sub>2</sub> and Ni/Ce<sub>0.75</sub>Zr<sub>0.25</sub>O<sub>2</sub> (IMP) catalysts. These values attained approach the equilibrium values as reported elsewhere (Zhu and Flytzani-Stephanopoulos, 2001). In contrast, about 60% CH<sub>4</sub> conversion and 80% CO selectivity were achieved over 5 wt% Ni/ZrO<sub>2</sub> (IMP) catalyst at the same reaction temperature. This indicates that 5 wt% Ni/CeO<sub>2</sub> and Ni/Ce<sub>0.75</sub>Zr<sub>0.25</sub>O<sub>2</sub> (IMP) catalysts give higher MPO catalytic activity and selectivity to synthesis gas than those of 5 wt% Ni/ZrO<sub>2</sub> (IMP) catalyst.

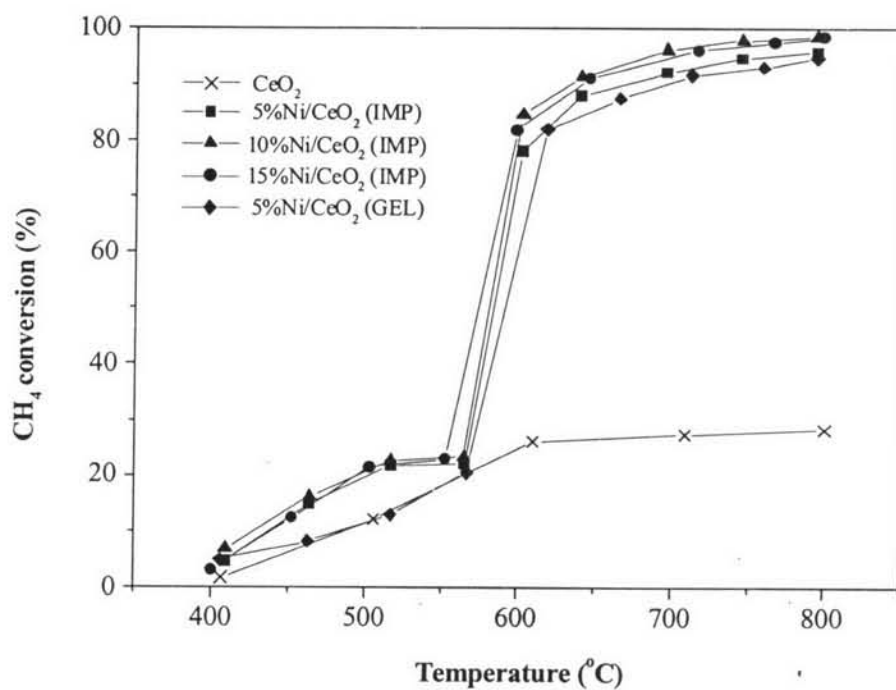
With increasing Ni loading, the CH<sub>4</sub> conversion over Ni/CeO<sub>2</sub> and Ni/Ce<sub>0.75</sub>Zr<sub>0.25</sub>O<sub>2</sub> (IMP) catalysts was insignificantly increased (ca. 2%) whereas CO and H<sub>2</sub> selectivities were remained unchanged. For Ni/ZrO<sub>2</sub> (IMP) catalyst, the CH<sub>4</sub> conversion, CO and H<sub>2</sub> selectivities were considerably increased when

increasing Ni loading from 5 to 10 wt% but were insignificantly altered after which the Ni loading was increased to 15 wt%. This may be due to the fact that CH<sub>4</sub> conversion, CO and H<sub>2</sub> selectivities approach the equilibrium values. At this point, the change in catalytic activity by catalyst would be less pronounced. Therefore, no effect could be observed as for the change in Ni loading.

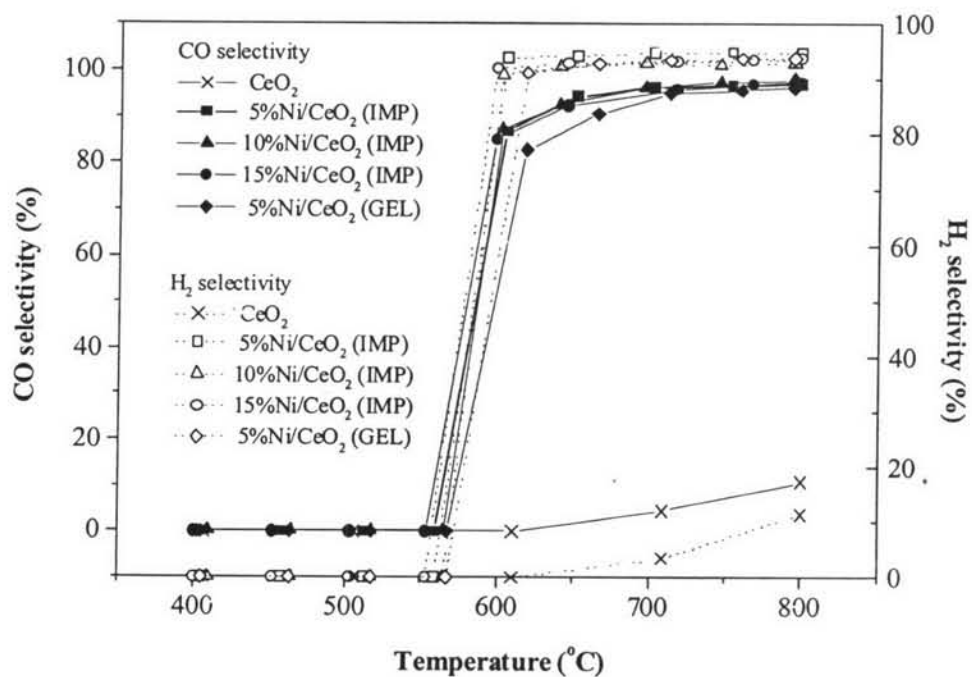
The results indicated that the IMP catalysts are more active than GEL catalysts, as can also be seen in Figures 4.5–4.7. It is believed that the decomposition of methane occurs on the metal (Noronha *et al.*, 2001). The low activity of the catalysts prepared by gel impregnation method can be attributed to a lower degree of dispersion of metal compared to that of the catalysts prepared by impregnation method.

The CH<sub>4</sub>/O<sub>2</sub> ratio also affects the catalytic activity of the catalysts. As given in Table 4.2, an increase in oxygen content in the feed stream (CH<sub>4</sub>/O<sub>2</sub> = 1.6) resulted in decreasing CO and H<sub>2</sub> selectivities but retaining the CH<sub>4</sub> conversion. In the case of insufficient oxygen (CH<sub>4</sub>/O<sub>2</sub> = 2.5), the CH<sub>4</sub> conversion was found to decrease for 15wt%Ni/ZrO<sub>2</sub> (IMP) catalyst while it remained unchanged for 15wt%Ni/CeO<sub>2</sub> and 15wt%Ni/Ce<sub>0.75</sub>Zr<sub>0.25</sub>O<sub>2</sub> (IMP) catalysts. The CO and H<sub>2</sub> selectivities were slightly increased with an increase in CH<sub>4</sub>/O<sub>2</sub> ratio. This might be due to that CeO<sub>2</sub> and Ce<sub>0.75</sub>Zr<sub>0.25</sub>O<sub>2</sub> have considerable oxygen storage ability (Fornasiero *et al.*, 1995; Fornasiero *et al.*, 1996; Otsuka *et al.*, 1998). Evidence of carbon formation was found at the CH<sub>4</sub>/O<sub>2</sub> feed ratio of 2.5, indicated by the H<sub>2</sub>/CO ratio above 2.0 (Pantu and Gavalas, 2002).



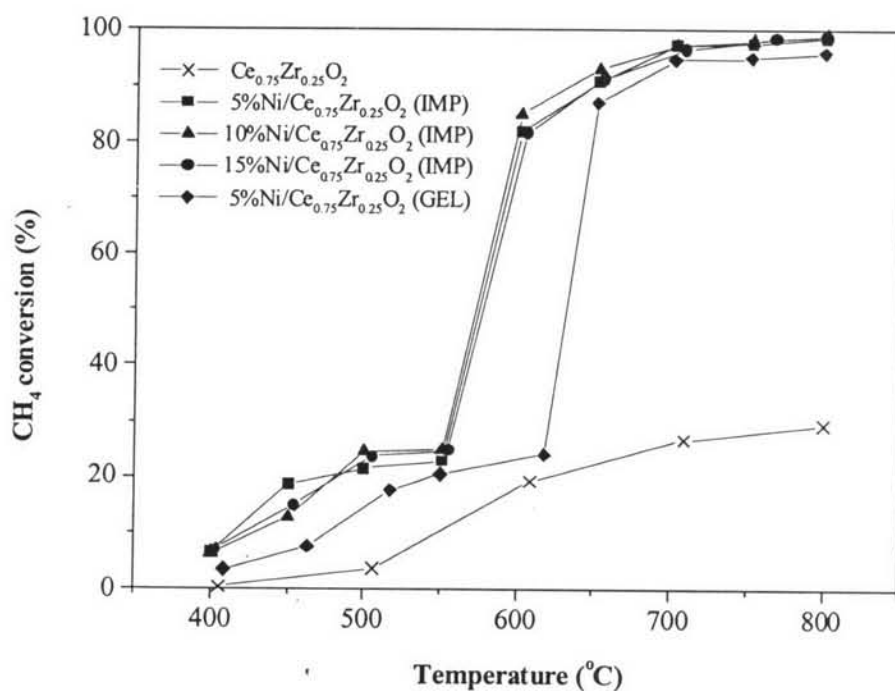


(a)

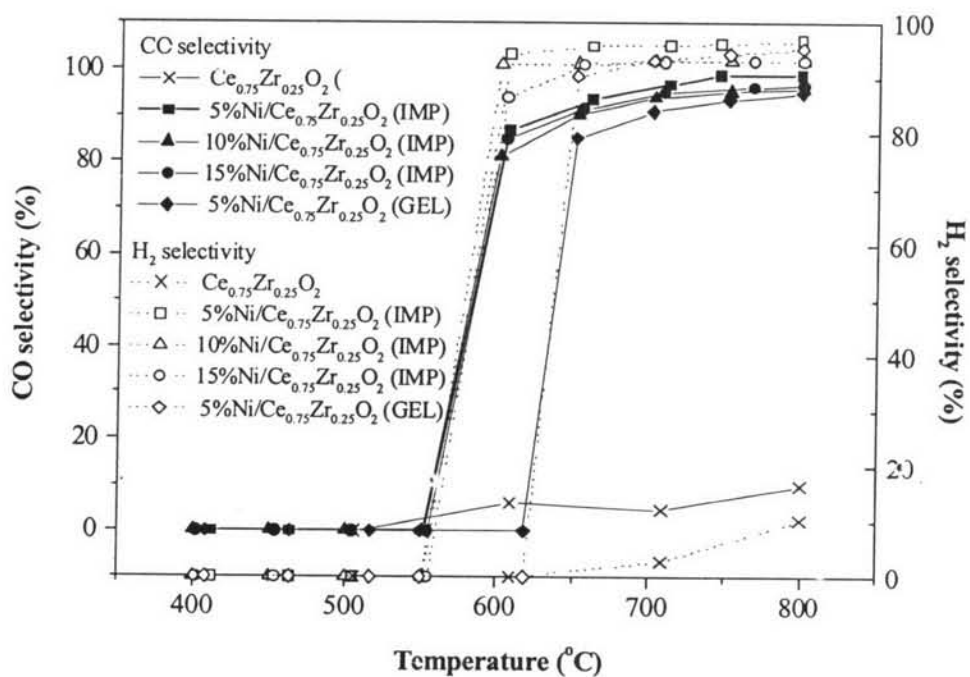


(b)

**Figure 4.5** The CH<sub>4</sub> conversion (a), CO selectivity and H<sub>2</sub> selectivity (b) of methane partial oxidation over Ni/CeO<sub>2</sub> catalysts calcined at 500°C (CH<sub>4</sub>/O<sub>2</sub> ratio of 2.0, GHSV = 53,000 hr<sup>-1</sup>).

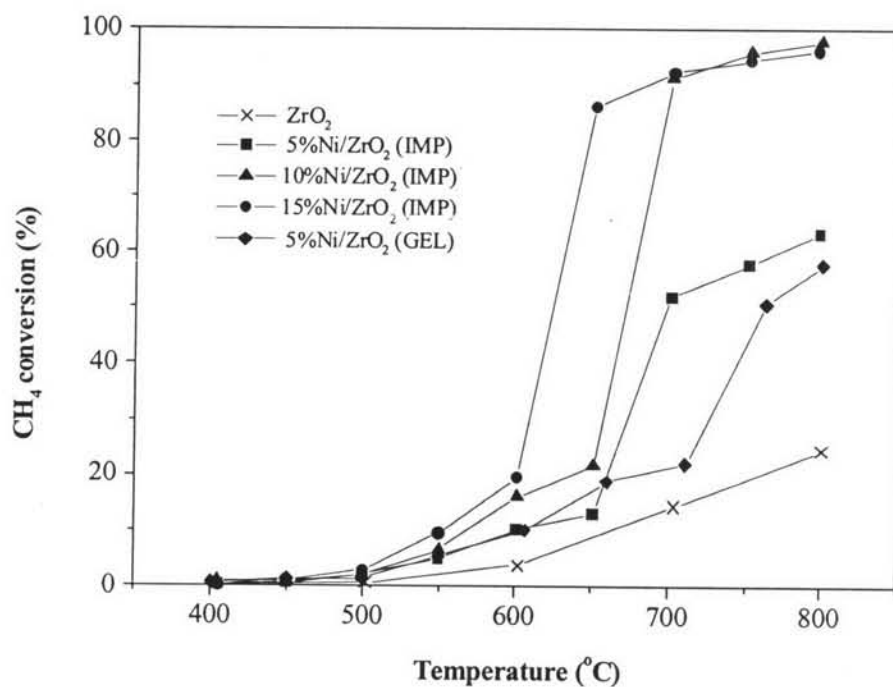


(a)

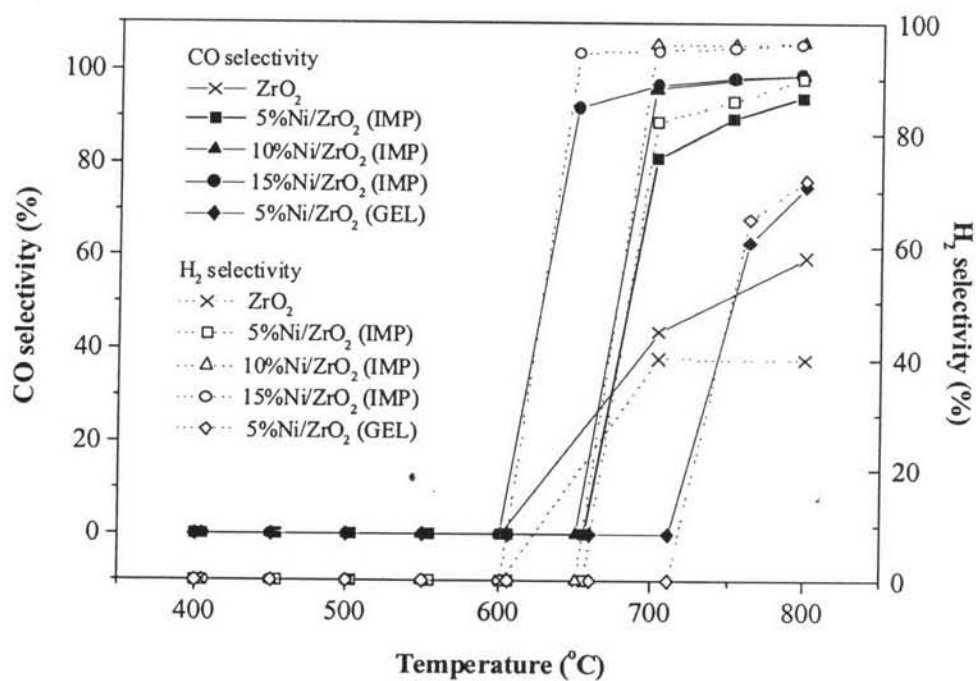


(b)

**Figure 4.6** The CH<sub>4</sub> conversion (a), CO selectivity and H<sub>2</sub> selectivity (b) of methane partial oxidation over Ni/Ce<sub>0.75</sub>Zr<sub>0.25</sub>O<sub>2</sub> catalysts calcined at 500°C (CH<sub>4</sub>/O<sub>2</sub> ratio of 2.0, GHSV = 53,000 hr<sup>-1</sup>).



(a)



(b)

**Figure 4.7** The CH<sub>4</sub> conversion (a), CO selectivity and H<sub>2</sub> selectivity (b) of methane partial oxidation over Ni/ZrO<sub>2</sub> catalysts calcined at 500°C (CH<sub>4</sub>/O<sub>2</sub> ratio of 2.0, GHSV = 53,000 hr<sup>-1</sup>).

**Table 4.2** Methane partial oxidation on 0.1 g of 15%Ni/CeO<sub>2</sub> (IMP), 15%Ni/Ce<sub>0.75</sub>Zr<sub>0.25</sub>O<sub>2</sub> (IMP) or 15%Ni/ZrO<sub>2</sub> (IMP) catalysts using varied CH<sub>4</sub>/O<sub>2</sub> feed at 100 ml/min flow rate (GHSV = 53,000 hr<sup>-1</sup>)

Temperature (°C)	CH <sub>4</sub> /O <sub>2</sub> Feed ratio	15%Ni/CeO <sub>2</sub>				15%Ni/Ce <sub>0.75</sub> Zr <sub>0.25</sub> O <sub>2</sub>				15%Ni/ZrO <sub>2</sub>			
		X <sub>CH<sub>4</sub></sub> (%)	S <sub>CO</sub> (%)	S <sub>H<sub>2</sub></sub> (%)	H <sub>2</sub> /CO	X <sub>CH<sub>4</sub></sub> (%)	S <sub>CO</sub> (%)	S <sub>H<sub>2</sub></sub> (%)	H <sub>2</sub> /CO	X <sub>CH<sub>4</sub></sub> (%)	S <sub>CO</sub> (%)	S <sub>H<sub>2</sub></sub> (%)	H <sub>2</sub> /CO
700	2.5	94	97	93	2.4	94	98	95	2.4	84	97	96	2.2
750	2.5	95	98	93	2.4	97	99	96	2.4	87	98	97	2.2
800	2.5	96	98	94	2.4	97	99	96	2.4	88	99	98	2.2
700	2.0	95	96	92	2.0	96	96	93	2.0	92	96	95	2.0
750	2.0	97	97	93	2.0	97	97	94	2.0	94	97	96	2.0
800	2.0	98	98	93	2.0	98	98	95	2.0	96	98	96	2.0
700	1.6	98	91	90	2.0	97	91	91	2.0	91	84	88	2.0
750	1.6	99	92	90	2.0	98	93	91	2.0	95	89	90	2.0
800	1.6	99	93	90	2.0	98	94	91	2.0	96	91	90	2.0

*Note:* The oxygen was completely consumed at all these cases.

#### 4.4.2.2 Carbon Formation

It was also observed that at a low Ni loading all catalysts are rather stable over a 24 hr period of time on stream as shown in Figure 4.8. Thus, to compare the effect of support on coke formation, the high Ni loading of 15 wt% was chosen. As can be seen from Figure 4.9, the 15 wt% Ni/ZrO<sub>2</sub> (IMP) catalyst possesses the least stability. However, the H<sub>2</sub>/CO ratio of the catalysts is rather constant.

TPO technique was used to quantify the amount of carbon formation on the spent catalysts. The TPO profiles of the spent 15 wt%Ni/CeO<sub>2</sub> (IMP), 15 wt%Ni/Ce<sub>0.75</sub>Zr<sub>0.25</sub>O<sub>2</sub> (IMP) and 15 wt%Ni/ZrO<sub>2</sub> (IMP) catalysts are shown in Figure 4.10. The TPO profiles show a large peak centered at ca. 650°C for the formers and at ca.700°C for the latter, with an additional peak centered at the temperature of 550°C. The two peaks observed on the TPO profile of 15wt%Ni/ZrO<sub>2</sub> (IMP) catalyst can be due to the presence of either different types of carbon or different sites where carbon is deposited. The results are confirmed by TEM images as shown in Figure 4.11. For spent Ni/CeO<sub>2</sub> and Ni/Ce<sub>0.75</sub>Zr<sub>0.25</sub>O<sub>2</sub> catalysts, it was observed that the only type of carbon deposition is in the form of filaments. The carbon structure is graphitic with the usual constant spacing between layers. The dark particle in the end of tube would be the encapsulated Ni species. For spent Ni/ZrO<sub>2</sub> catalyst, carbon nanotubes and graphite filaments were observed. The total amounts of carbon deposition on the spent catalysts are given in Table 4.3. The amount of carbon deposition was found in the order 15 wt% Ni/Ce<sub>0.75</sub>Zr<sub>0.25</sub>O<sub>2</sub> (IMP) < 15 wt% Ni/ZrO<sub>2</sub> (IMP) < 15 wt% Ni/CeO<sub>2</sub> (IMP) indicating that Ce<sub>0.75</sub>Zr<sub>0.25</sub>O<sub>2</sub> can promote the oxidation of the carbon. This was also conformed by the CH<sub>4</sub>-TPR experiments (Figure 4.12-4.14), revealing that the Ni/Ce<sub>0.75</sub>Zr<sub>0.25</sub>O<sub>2</sub> catalyst can produce CO<sub>2</sub> more than can Ni/ZrO<sub>2</sub> and Ni/CeO<sub>2</sub> catalysts. It is also concluded that Ni/Ce<sub>0.75</sub>Zr<sub>0.25</sub>O<sub>2</sub> has a higher surface oxygen mobility (Zhu and Flytzani-Stephanopoulos, 2001).

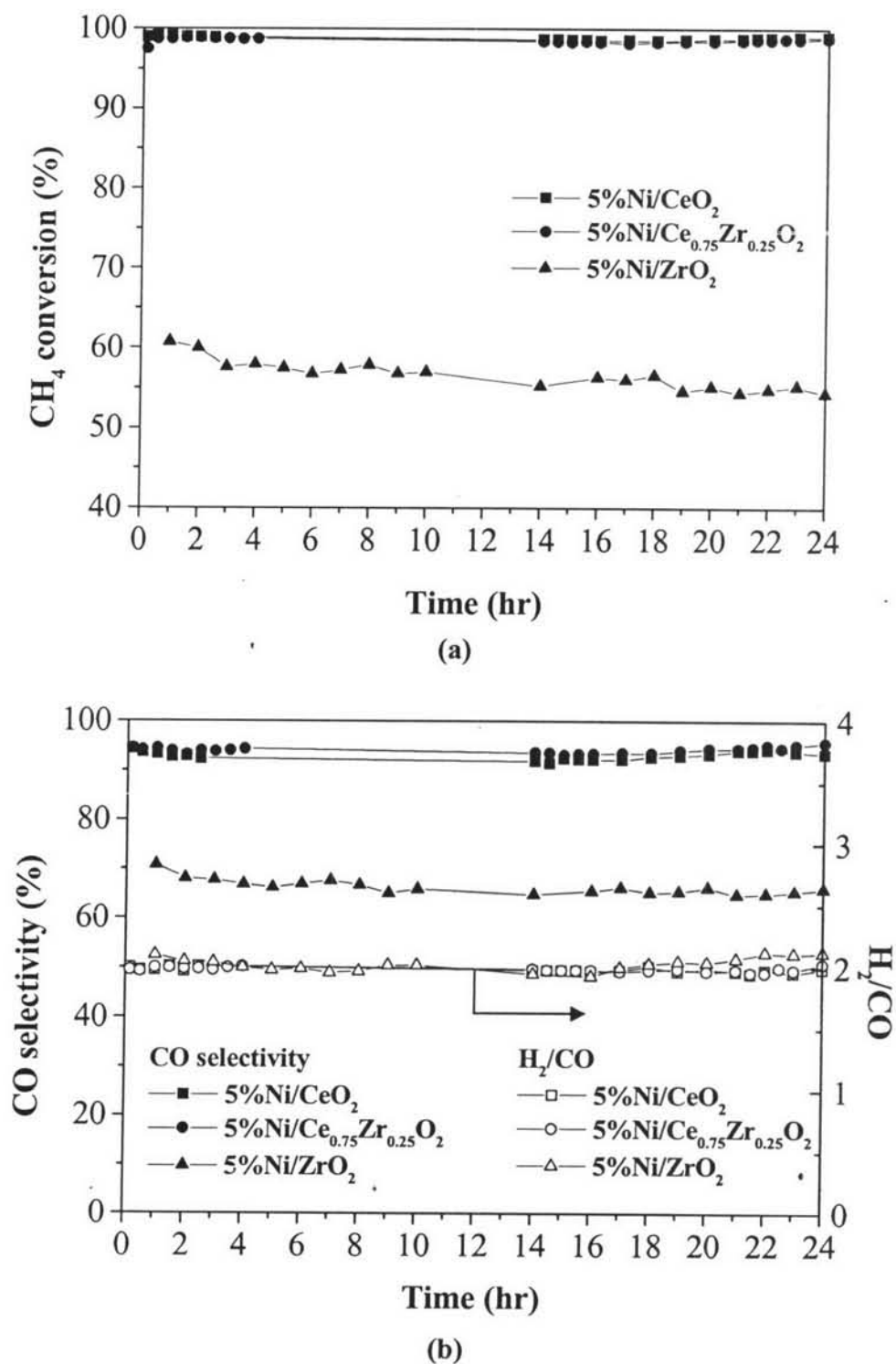


**Figure 4.8** The CH<sub>4</sub> conversion (a), CO selectivity and H<sub>2</sub>/CO (b) as a function of time over the 5 wt% Ni supported catalysts at 750°C (CH<sub>4</sub>/O<sub>2</sub> ratio of 2.0, GHSV = 53,000 hr<sup>-1</sup>).

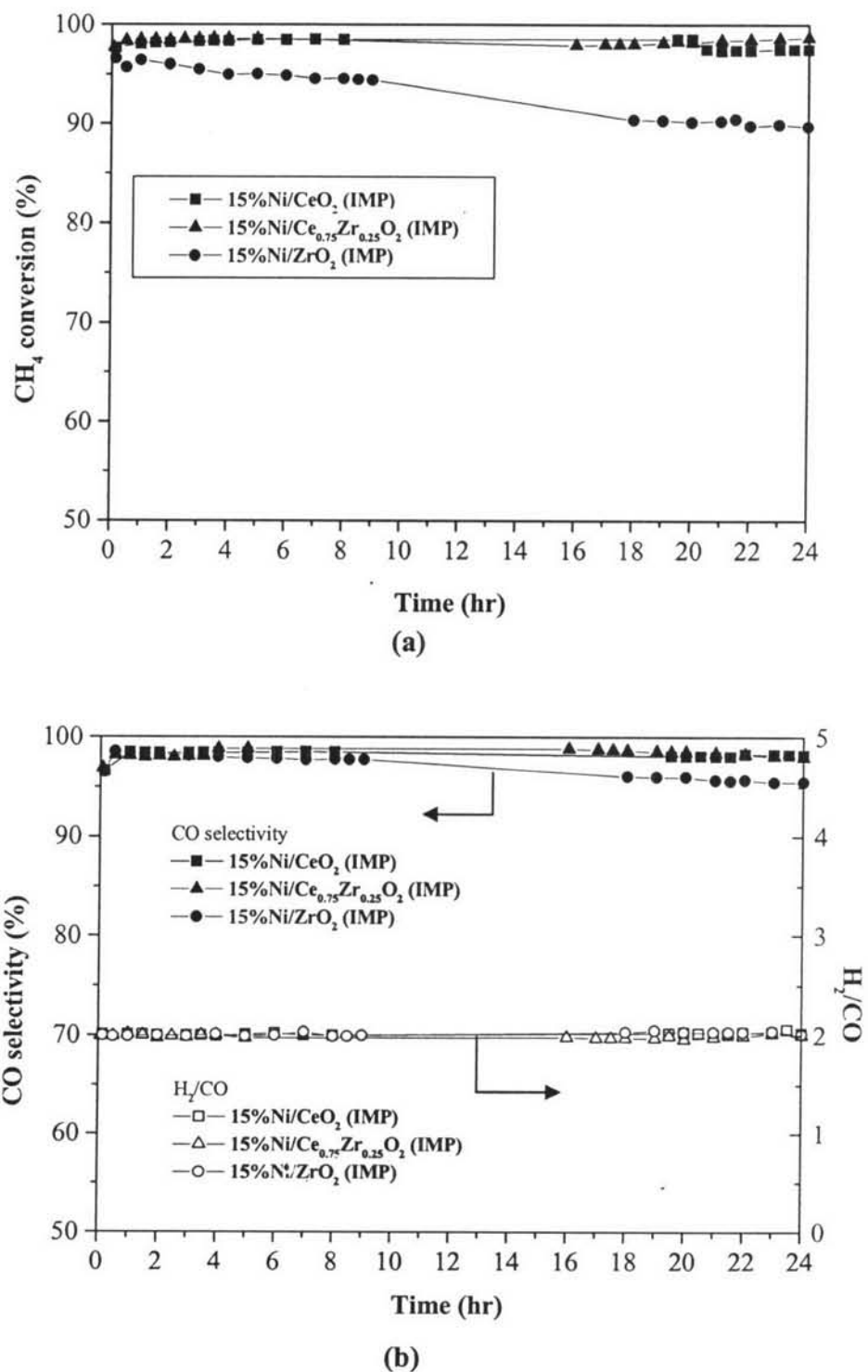


**Figure 4.9** The CH<sub>4</sub> conversion (a), CO selectivity and H<sub>2</sub>/CO (b) as a function of time over the 15 wt% Ni supported catalysts at 750°C (CH<sub>4</sub>/O<sub>2</sub> ratio of 2.0, GHSV = 53,000 hr<sup>-1</sup>).

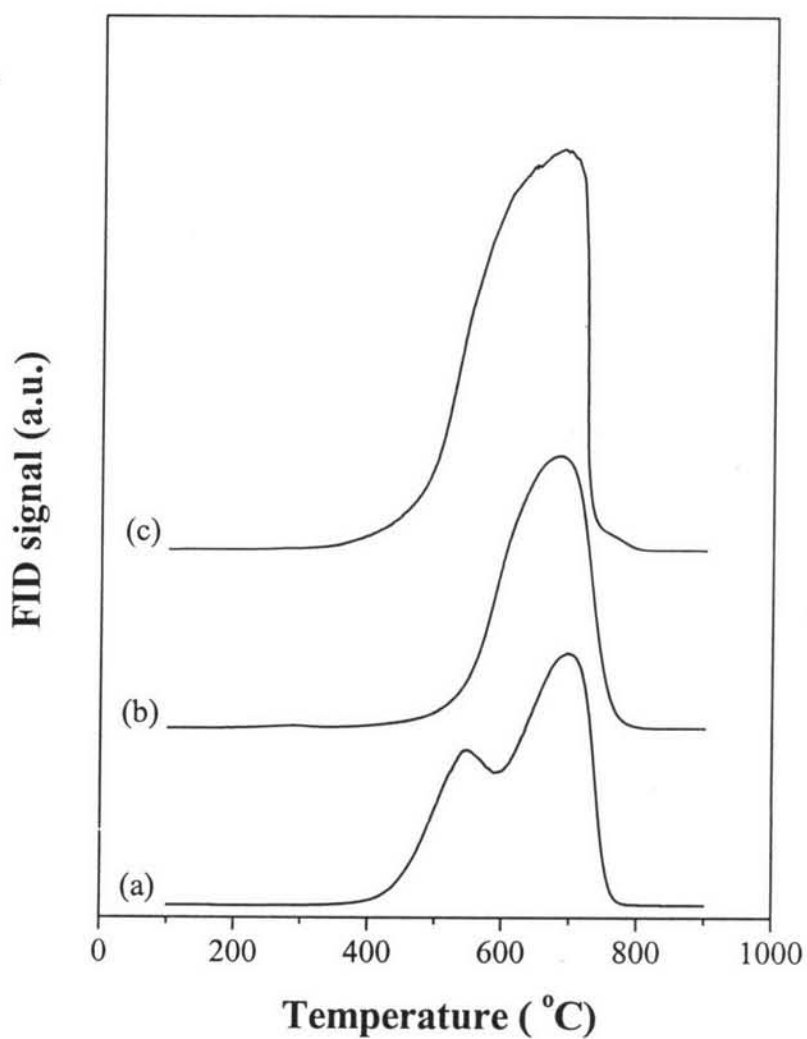


**Figure 4.10** TPO profiles of catalysts after exposure to MPO reaction at 750°C ( $\text{CH}_4/\text{O}_2 = 2.5$ ,  $\text{GHSV} = 53,000 \text{ hr}^{-1}$ ) for 4 hr with a heating rate of  $10^\circ\text{C min}^{-1}$ , an oxidizing gas containing 2% oxygen in He with a flow rate of  $40 \text{ ml min}^{-1}$ : (a) 15wt% Ni/ $\text{CeO}_2$  (IMP) (b) 15wt% Ni/ $\text{Ce}_{0.75}\text{Zr}_{0.25}\text{O}_2$  (IMP) (c) 15wt% Ni/ $\text{ZrO}_2$  (IMP).



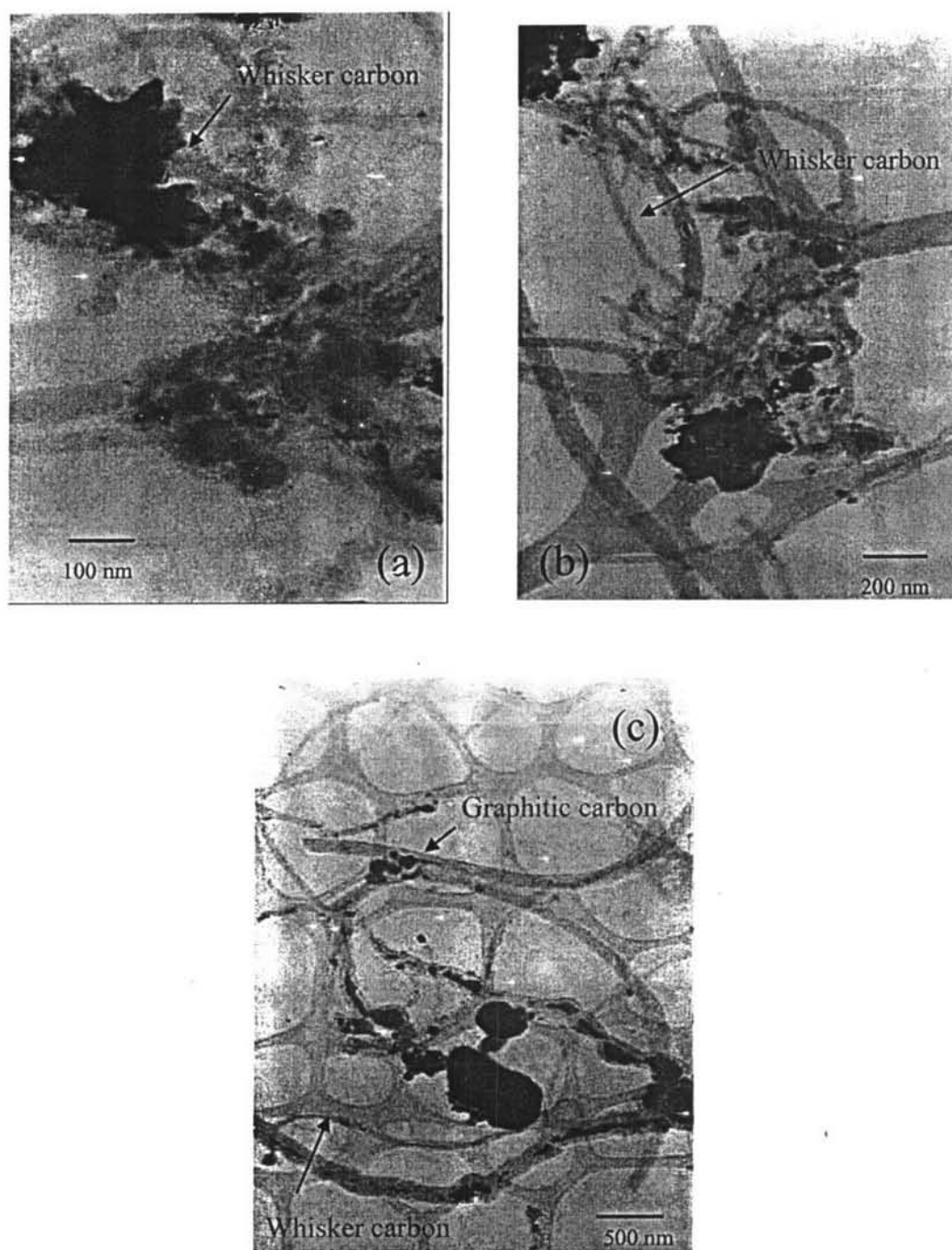


**Figure 4.11** TEM images of spent catalysts after exposure to MPO reaction at 750°C ( $\text{CH}_4/\text{O}_2 = 2.5$ ,  $\text{GHSV} = 53,000 \text{ hr}^{-1}$ ) for 4 hr: (a) 15wt% Ni/CeO<sub>2</sub> (IMP) (b) 15wt% Ni/Ce<sub>0.75</sub>Zr<sub>0.25</sub>O<sub>2</sub> (IMP) (c) 15wt% Ni/ZrO<sub>2</sub> (IMP).

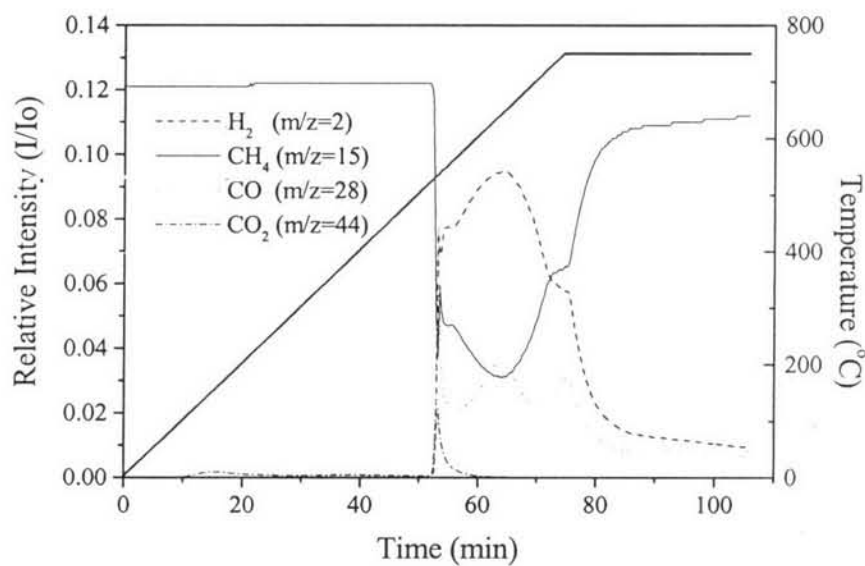
**Table 4.3** Amount of carbon deposition on the catalysts, as determined by TPO, using 2%O<sub>2</sub> in He and heating rate of 10°C/min.

Catalyst	CH <sub>4</sub> conversion <sup>a</sup> (%)	CO selectivity <sup>a</sup> (%)	H <sub>2</sub> selectivity <sup>a</sup> (%)	Percent of carbon (wt%)
5%Ni/CeO <sub>2</sub> (IMP) <sup>b</sup>	98	98	93	9.93
5%Ni/Ce <sub>0.75</sub> Zr <sub>0.25</sub> O <sub>2</sub> (IMP) <sup>b</sup>	98	99	96	8.56
5%Ni/ZrO <sub>2</sub> (IMP) <sup>b</sup>	74	98	97	4.18
10%Ni/CeO <sub>2</sub> (IMP) <sup>b</sup>	97	98	98	14.84
10%Ni/Ce <sub>0.75</sub> Zr <sub>0.25</sub> O <sub>2</sub> (IMP) <sup>b</sup>	97	98	98	10.61
10%Ni/ZrO <sub>2</sub> (IMP) <sup>b</sup>	90	96	96	12.11
15%Ni/CeO <sub>2</sub> (IMP) <sup>b</sup>	97	98	94	21.71
15%Ni/Ce <sub>0.75</sub> Zr <sub>0.25</sub> O <sub>2</sub> (IMP) <sup>b</sup>	97	98	96	14.09
15%Ni/ZrO <sub>2</sub> (IMP) <sup>b</sup>	94	95	97	16.94
15%Ni/CeO <sub>2</sub> (IMP) <sup>c</sup>	95	98	93	22.70
15%Ni/Ce <sub>0.75</sub> Zr <sub>0.25</sub> O <sub>2</sub> (IMP) <sup>c</sup>	97	99	96	12.87
15%Ni/ZrO <sub>2</sub> (IMP) <sup>c</sup>	87	98	97	15.82

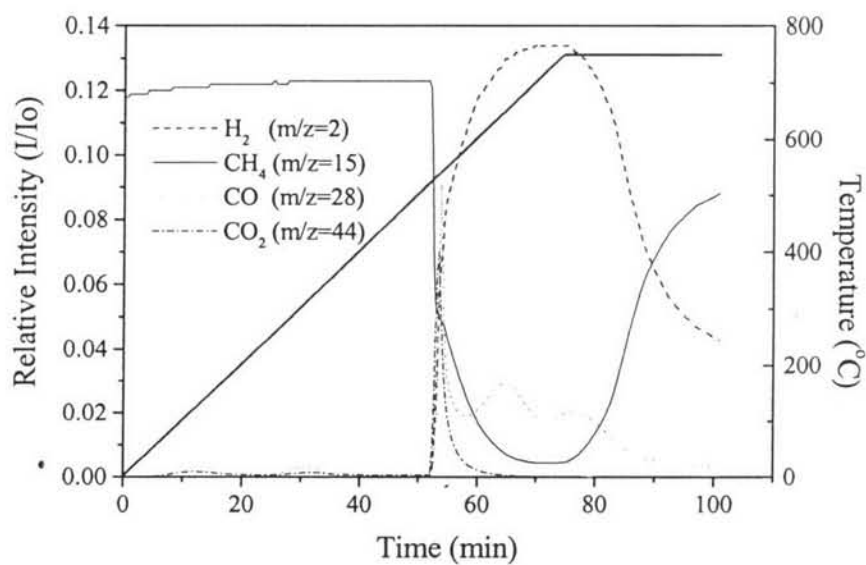
<sup>a</sup> measured at the end of reaction time

<sup>b</sup> after 24 hr reaction at 750°C and CH<sub>4</sub>/O<sub>2</sub> ratio of 2.0

<sup>c</sup> after 4 hr reaction at 750°C and CH<sub>4</sub>/O<sub>2</sub> ratio of 2.5

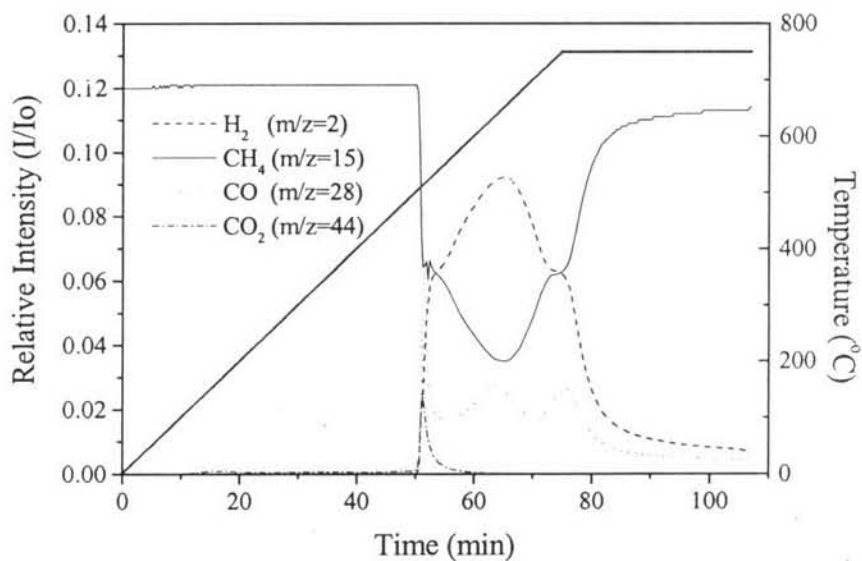


(a)

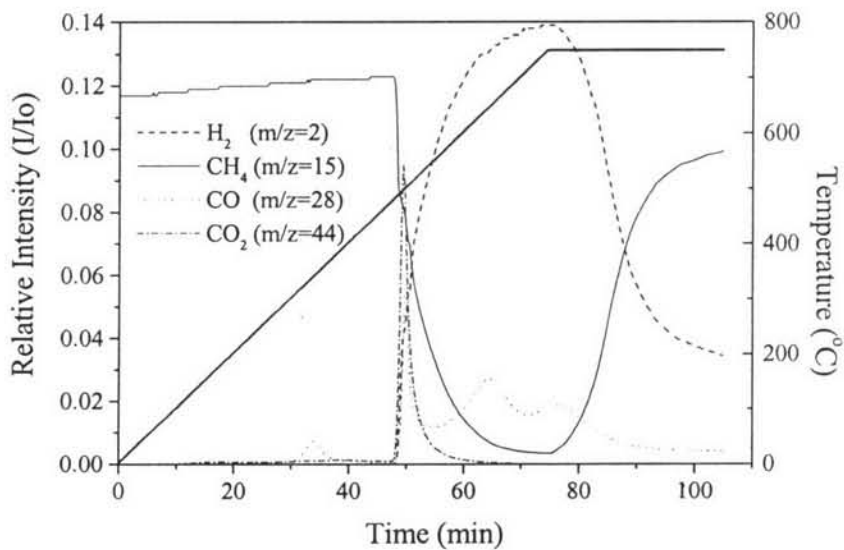


(b)

**Figure 4.12** CH<sub>4</sub>-TPR profiles of Ni/CeO<sub>2</sub> (IMP) catalysts calcined at 500°C with a heating rate of 10°C min<sup>-1</sup>, a reducing gas containing 2% methane in He with a flow rate of 50 ml min<sup>-1</sup>: (a) 5 wt% Ni/CeO<sub>2</sub> (IMP) (b) 15 wt% Ni/CeO<sub>2</sub> (IMP).

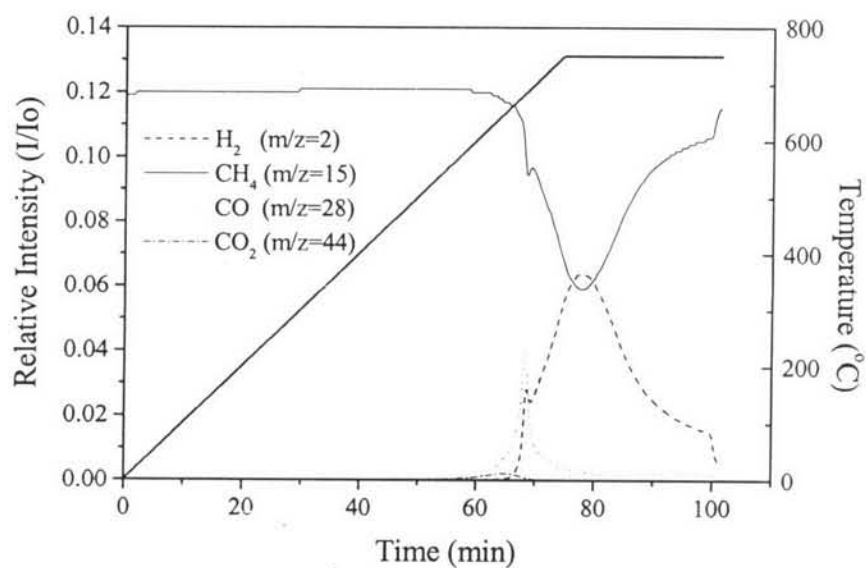


(a)

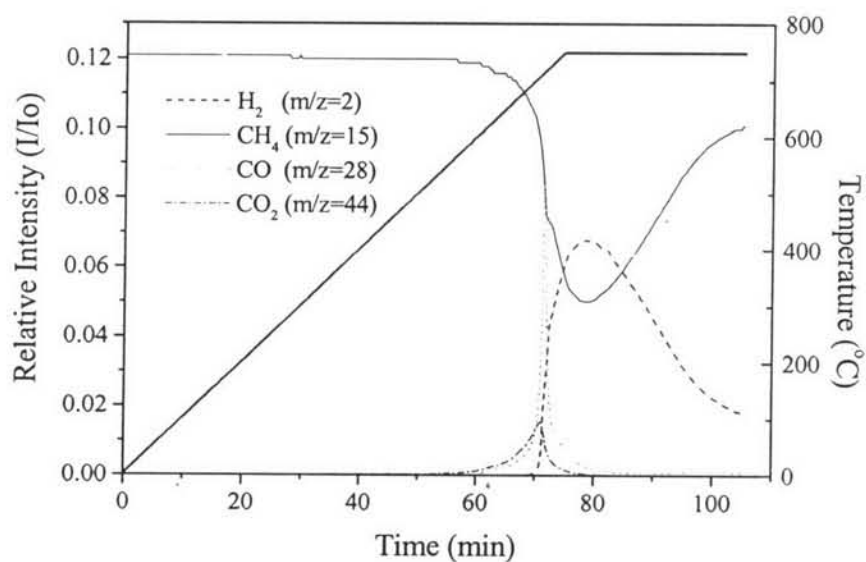


(b)

**Figure 4.13** CH<sub>4</sub>-TPR profiles of Ni/Ce<sub>0.75</sub>Zr<sub>0.25</sub>O<sub>2</sub> (IMP) catalysts calcined at 500°C with a heating rate of 10°C min<sup>-1</sup>, a reducing gas containing 2% methane in He with a flow rate of 50 ml min<sup>-1</sup>: (a) 5 wt% Ni/Ce<sub>0.75</sub>Zr<sub>0.25</sub>O<sub>2</sub> (IMP) (b) 15 wt% Ni/Ce<sub>0.75</sub>Zr<sub>0.25</sub>O<sub>2</sub> (IMP).



(a)



(b)

**Figure 4.14** CH<sub>4</sub>-TPR profiles of Ni/ZrO<sub>2</sub> catalysts calcined at 500°C with a heating rate of 10°C min<sup>-1</sup>, a reducing gas containing 2% methane in He with a flow rate of 50 ml min<sup>-1</sup>: (a) 5 wt% Ni/ZrO<sub>2</sub> (IMP) (c) 15 wt% Ni/ZrO<sub>2</sub> (IMP).

The coke formation on these catalysts is due to the methane decomposition since the TPO profiles are rather analogous as shown in Figure 4.15-4.16. The TPO profiles of methane decomposition over 15 wt% Ni/CeO<sub>2</sub> (IMP), 15 wt% Ni/Ce<sub>0.75</sub>Zr<sub>0.25</sub>O<sub>2</sub> (IMP) and 15 wt% Ni/ZrO<sub>2</sub> (IMP) exhibit a large peak centered at ca. 600-700°C with an additional peak centered at 550°C for 15 wt% Ni/ZrO<sub>2</sub> (IMP) catalyst. On the contrary, the TPO profiles of CO disproportionation over 15 wt% Ni/CeO<sub>2</sub> (IMP), 15 wt% Ni/Ce<sub>0.75</sub>Zr<sub>0.25</sub>O<sub>2</sub> (IMP) and 15 wt% Ni/ZrO<sub>2</sub> (IMP) catalysts exhibit a peak centered at ca. 300-400°C.

#### 4.5 Conclusions

It can be concluded that the catalysts prepared by impregnation method showed higher catalytic activity for methane partial oxidation than those prepared by gel impregnation method due to a better metallic Ni dispersion and reducibility. The Ni/CeO<sub>2</sub> and Ni/Ce<sub>0.75</sub>Zr<sub>0.25</sub>O<sub>2</sub> catalysts showed higher catalytic activity for methane partial oxidation than Ni/ZrO<sub>2</sub> catalyst. The H<sub>2</sub>/CO molar ratio of 2.0 was achieved at a CH<sub>4</sub>/O<sub>2</sub> ratio of 2.0 for all catalysts. The effect of CH<sub>4</sub>/O<sub>2</sub> ratio on the activity and H<sub>2</sub>/CO was more pronounced with Ni/ZrO<sub>2</sub> than Ni/CeO<sub>2</sub> and Ni/Ce<sub>0.75</sub>Zr<sub>0.25</sub>O<sub>2</sub> catalysts. The CH<sub>4</sub> conversion slightly increased while CO and H<sub>2</sub> selectivities remained unchanged with increasing Ni loading for Ni/CeO<sub>2</sub> and Ni/Ce<sub>0.75</sub>Zr<sub>0.25</sub>O<sub>2</sub> catalysts. The Ni/Ce<sub>0.75</sub>Zr<sub>0.25</sub>O<sub>2</sub> catalyst showed the highest stability with a little carbon deposition after prolonged reaction time. The carbon on the surface of the catalyst was due mainly to the methane decomposition.

#### 4.6 Acknowledgments

The authors would like to thank RGJ, Ph.D. program, Thailand Research Fund for the financial support. We acknowledge Dr. Toranin Chairuangstri of Electron Microscope Centre, Chaingmai University for his assistance on TEM analysis.

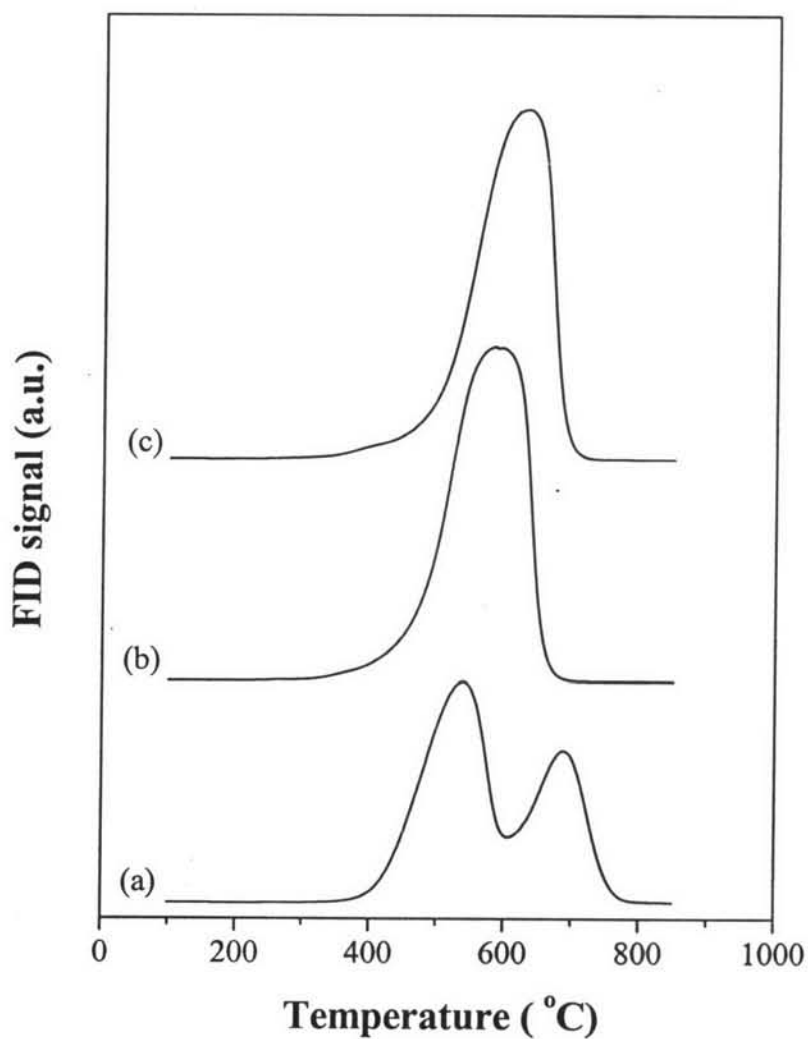


**Figure 4.15** TPO profiles of catalysts after exposure to 2%CH<sub>4</sub> in He at 750°C for 1 hr with a heating rate of 10°C min<sup>-1</sup>, an oxidizing gas containing 2% oxygen in He with a flow rate of 40 ml min<sup>-1</sup>: (a) 15wt% Ni/CeO<sub>2</sub> (IMP) (b) 15wt% Ni/Ce<sub>0.75</sub>Zr<sub>0.25</sub>O<sub>2</sub> (IMP) (c) 15wt% Ni/ZrO<sub>2</sub> (IMP).

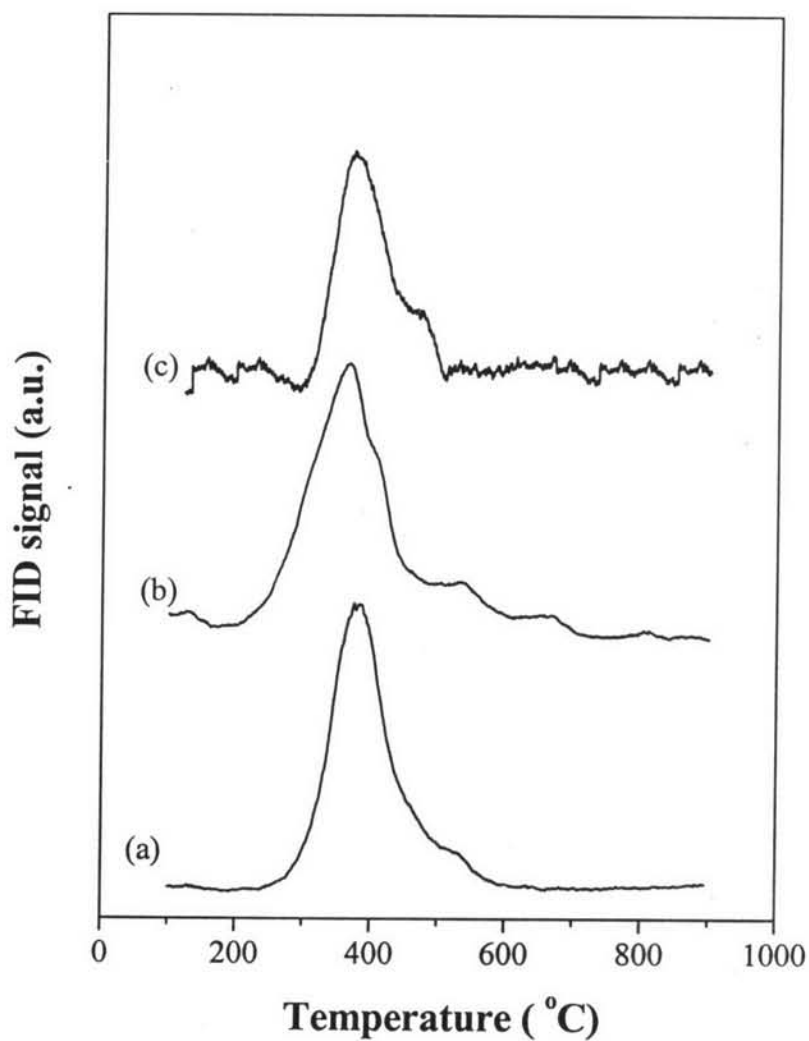


**Figure 4.16** TPO profiles of catalysts after exposure to 1%CO in He at 750°C for 1 hr with a heating rate of 10°C min<sup>-1</sup>, an oxidizing gas containing 2% oxygen in He with a flow rate of 40 ml min<sup>-1</sup>: (a) 15wt% Ni/CeO<sub>2</sub> (IMP) (b) 15wt% Ni/Ce<sub>0.75</sub>Zr<sub>0.25</sub>O<sub>2</sub> (IMP) (c) 15wt% Ni/ZrO<sub>2</sub> (IMP).



#### 4.7 References

- Au, C.T., Wang, H.Y., and Wan, H.L. (1996) Mechanistic Studies of CH<sub>4</sub>/O<sub>2</sub> Conversion over SiO<sub>2</sub>-Supported Nickel and Copper Catalysts. Journal of Catalysis, 158, 343.
- Boucouvalas, Y., Zhang, Z., Verykios, X.E. (1994) Heat Transport Limitations and Reaction Scheme of Partial Oxidation of Methane to Synthesis gas over supported Rhodium Catalysts. Catalysis Letters, 27, 131.
- Boucouvalas, Y., Zhang, Z., Verykios, X.E. (1996) Partial Oxidation of Methane to Synthesis Gas via Direct Reaction Scheme over Ru/TiO<sub>2</sub> Catalyst. Catalysis Letters, 40, 189.
- Chellappa, A.S., and Viswanath D.S. (1995) Partial Oxidation of Methane using Ferric Molybdate Catalyst. Industrial Engineering Chemistry Research, 34, 1933.
- Dissanayake, D., Rosynek, M.P., Kharas, K.C.C., and Lunsford, J.H. (1991) Partial Oxidation of Methane to Carbon monoxide and Hydrogen over a Ni/Al<sub>2</sub>O<sub>3</sub> Catalyst. Journal of Catalysis, 132, 117.
- Dong, W., Jun, K., Roh, H., Liu, Z., and Park, S. (2002) Comparative Study on Partial Oxidation of Methane over Ni/ZrO<sub>2</sub>, Ni/CeO<sub>2</sub> and Ni/Ce-ZrO<sub>2</sub> Catalysts. Catalysis Letters, 78, 215.
- Fornasiero, P., Monte, D.R., Ranga, G.R., Kaspar, J., Meriani, S., Trovarelli, A., and Graziani, M. (1995) Rh-loaded CeO<sub>2</sub>-ZrO<sub>2</sub> Solid Solutions as Highly Efficient Oxygen Exchangers: Dependence of the Reduction Behavior and the Oxygen Storage Capacity on the Structural Properties. Journal of Catalysis, 151, 168.
- Fornasiero, P., Balducci, G., Monte, R.D., Kaspar, J., Sergio, V., Gubitosa, G., Ferrero, A., Graziani, M. (1996) Modification of the Redox Behaviour of CeO<sub>2</sub> induced by Structural doping with ZrO<sub>2</sub>. Journal of Catalysis, 164, 173.
- Gonzalez-Velasco, J.R., Gutierrez-Ortiz, A.M., Jean-Louis, M., Botas, A.J., Gonzalez-Marcos, P.M., and Blanchard, G. (1999) Contribution of

- Cerium/Zirconium Mixed Oxides to the Activity of a New Generation of TWC. Applied Catalysis B: Environmental, 22, 167.
- Hargreaves, S.J., Graham, J.H., Richard, J.W. (1990) Control of Product selectivity in the Partial Oxidation of Methane. Letters to Nature, 348, 428.
- Hickman, D.A., and Schmidt L.D. (1993) Production of Syngas by Direct Catalytic Oxidation of Methane. Science, 259, 343.
- Hori, C.E., Permana, H., Simon Ng, K.Y., Brenner, A., More, K., Rahmoeller, K.M., and Belton, D. (1998) Thermal Stability of Oxygen Storage Properties in a Mixed  $\text{CeO}_2\text{-ZrO}_2$  System. Applied Catalysis B: Environmental, 16 (1998) 105.
- Hu Y.H., Ruckenstein E. (1996) Transient Kinetic Studies of Partial Oxidation of  $\text{CH}_4$ . Journal of Catalysis, 158, 260.
- Irigoyen, B., Castellani, N., Juan, A. (1998) Methane Oxidation reactions on  $\text{MoO}_3(100)$ : A Theoretical Study, Journal of Molecular Catalysis A: Chemical, 129, 297.
- Lu, Y., Xue, J., Yu, C., Liu, Y., and Shen, S. (1998) Mechanistic Investigations on the Partial Oxidation of Methane to Synthesis Gas over a Nickel-on-Alumina Catalyst. Applied Catalysis A: General, 174, 121.
- Mallens, E.P.J., Hoebink J.H.B.J., and Marin G.B. (1997) The Reaction Mechanism of the Partial Oxidation of Methane to Synthesis Gas: A Transient Kinetic Study over Rhodium and a Comparison with Platinum. Journal of Catalysis, 167, 43.
- Miao, Q. Xiong, G., Sheng, S., Cui, W., Xu, L., and Guo, X. (1997) Partial Oxidation of Methane to Syngas over Nickel-based Catalysts Modified by Alkali Metal Oxide and Rare Earth Metal Oxide. Applied Catalysis A: General, 154, 17.
- Montoya, J.A., Romero-Pascual, E., Gimón, C., Del Angle, P., Monzon, A., (2000) Methane Reforming with  $\text{CO}_2$  over  $\text{Ni/ZrO}_2\text{-CeO}_2$  Catalysts Prepared by Sol-Gel. Catalysis Today, 63, 71.
- Noronha, F.B., Fendley, E.C., Soares, R.R., Alvarez, W.E., Resasco, D.E. (2001) Correlation Between Catalytic Activity and Support Reducibility in the  $\text{CO}_2$

- Reforming of Methane over Pt/Ce<sub>x</sub>Zr<sub>1-x</sub>O<sub>2</sub> Catalysts. Chemical Engineering Journal, 82, 21.
- Otsuka, K., Wang, Y., Sunada, E., and Yamanaka, I. (1998) Direct Partial Oxidation of Methane to Synthesis Gas by Cerium Oxide. Journal of Catalysis, 175, 152.
- Otsuka, K., Wang, Y., and Nakamura, M. (1999) Direct Conversion of Methane to Synthesis Gas Through Reaction using CeO<sub>2</sub>-ZrO<sub>2</sub> Solid Solution at Moderate Temperature. Applied Catalysis A: General, 183, 317.
- Pantu, P., Kim, K., and Gavalas, G.R. (2000) Methane Partial Oxidation on Pt/CeO<sub>2</sub>-ZrO<sub>2</sub> in the Absence of Gaseous Oxygen. Applied Catalysis A: General, 193, 203.
- Pantu, P., and Gavalas, G.R. (2002) Methane Partial Oxidation on Pt/CeO<sub>2</sub> and Pt/Al<sub>2</sub>O<sub>3</sub> catalysts. Applied Catalysis A: General, 223, 253.
- Pengpanich, S., Meeyoo, V., Rirksomboon, T., and Bunyakiat, K. (2002) Catalytic Oxidation of Methane over CeO<sub>2</sub>-ZrO<sub>2</sub> Mixed Oxide Solid Solution Catalysts Prepared via Urea Hydrolysis. Applied Catalysis A: General, 234, 221.
- Roh, H., Jun, K., Dong, W., Chang, J., Park, S., and Joe, Y. (2002) Highly Active and Stable Ni/Ce-ZrO<sub>2</sub> Catalyst for H<sub>2</sub> Production from Methane. Journal of Molecular Catalysis A: Chemical, 181, 137.
- Ruckenstein, E., and Hu, Y.H. (1999) Methane Partial Oxidation over NiO/MgO Solid Solution Catalysts. Applied Catalysis A: General, 183, 85.
- Shishido, T., Sokenobu, M., Morioka, H., Kondo, M., Wang, Y., Takaki, K., Takehira, K., (2002) Partial Oxidation of Methane over Ni/Mg-Al Oxide Catalysts Prepared by Solid Phase Crystallization Method from Mg-Al Hydrotalcite-like Precursors. Applied Catalysis A: General, 223, 235.
- Stagg-Williams, S.M., Noranha, F.B., Fendley, G., Resasco, D.E. (2000) CO<sub>2</sub> Reforming of CH<sub>4</sub> over Pt/ZrO<sub>2</sub> Catalysts Promoted with La and Ce Oxides. Journal of Catalysis, 194, 240.
- Swann, H.M., Kroll, V.C.H., Martin, G.A., Mirodatos, C. (1994) Deactivation of Supported Nickel Catalysts during the Reforming of Methane by Carbon Dioxide. Catalysis Today, 21, 571.

- Takeguchi, T., Furukawa, S., and Inoue, M. (2001) Hydrogen Spillover from NiO to the Large Surface Area CeO<sub>2</sub>-ZrO<sub>2</sub> Solid Solutions and Activity of the NiO/CeO<sub>2</sub>-ZrO<sub>2</sub> Catalysts for Partial Oxidation of Methane. Journal of Catalysis, 202,14.
- Tang, S., Lin, J., and Tan, K.L. (1998) Partial Oxidation of Methane to Syngas over Ni/MgO, Ni/CaO and Ni/CeO<sub>2</sub>. Catalysis Letters, 51, 169.
- Tsang, S.C., Claridge, J.B., and Green, M.L.H. (1995) Recent Advances in the Conversion of Methane to Synthesis Gas. Catalysis Today, 23, 3.
- Zhu, T., and Flytzani-Stephanopoulos, M. (2001) Catalytic Partial Oxidation of Methane to Synthesis gas over Ni-CeO<sub>2</sub>. Applied Catalysis A: General, 208, 403.